UNCLASSIFIED

SECURITY CLASSIFICATION OF THIS PAGE (When Data Entered)

REPORT DOCUMENTATION PAGE

READ INSTRUCTIONS BEFORE COMPLETING FORM

1. REPORT NUMBER
NOSC Technical Report 878 (TR 878)

2. GOVT ACCESSION NO.

3. RECIPIENT'S CATALOG NUMBER

4. TITLE (and Subtitle)
FREE-SWIMMING SUBMERSIBLE HYDRODYNAMIC FAIRING DESIGN

5. TYPE OF REPORT & PERIOD COVERED
Interim Report
June–August 1982

6. PERFORMING ORG. REPORT NUMBER

7. AUTHOR(s)
D.M. Ladd

8. CONTRACT OR GRANT NUMBER(s)

9. PERFORMING ORGANIZATION NAME AND ADDRESS
Naval Ocean Systems Center
San Diego, CA 92152

10. PROGRAM ELEMENT, PROJECT, TASK AREA & WORK UNIT NUMBERS
FGOV, 521-MS31

11. CONTROLLING OFFICE NAME AND ADDRESS
U.S. Department of Interior
Geological Survey
Reston, VA 22092

12. REPORT DATE
1 June 1983

13. NUMBER OF PAGES
81

14. MONITORING AGENCY NAME & ADDRESS(if different from Controlling Office)

15. SECURITY CLASS. (of this report)
Unclassified

15a. DECLASSIFICATION/DOWNGRADING SCHEDULE

16. DISTRIBUTION STATEMENT (of this Report)

Distribution limited to US Government agencies only; operational or administrative purposes; 1 June 1983. Other requests for this document must be referred to NOSC.

17. DISTRIBUTION STATEMENT (of the abstract entered in Block 20, if different from Report)

18. SUPPLEMENTARY NOTES

19. KEY WORDS (Continue on reverse side if necessary and identify by block number)

Submersible
Hydrodynamics fairing
Free-swimming vehicle

20. ABSTRACT (Continue on reverse side if necessary and identify by block number)

This report describes the hydrodynamic design assistance provided by NOSC Code 6342 in the design of the hydrodynamic fairing for the NOSC Free-Swimming Submersible. The four specific areas of nose and tail shape, vehicle stability, vehicle drag and propulsion are addressed. It can be concluded that the vehicle is hydrodynamically stable over the intended speed range and that vehicle maximum speed can be increased from the present 1.8 knots to 5 knots with the addition of a hydrodynamic fairing.

DD FORM 1 JAN 73 1473 EDITION OF 1 NOV 65 IS OBSOLETE

S/N 0102-LF-014-6601

UNCLASSIFIED

SECURITY CLASSIFICATION OF THIS PAGE (When Data Entered)

CONTENTS

Nomenclature . . . page 3

1. Introduction . . . 9

2. Nose and Tail Shape . . . 11

3. Vehicle Stability . . . 18

4. Vehicle Drag . . . 30

5. Propulsion . . . 38

6. Conclusions . . . 45

7. References . . . 47

Appendix

ILLUSTRATIONS

1. NOSC Free-swimming Vehicle Concept, Testbed Configuration . . . page 10

2. Free Swimming Submersible, Compact Configuration . . . 10

3. Potential Flow and Body Radius versus X/L, for Final Body Shape . . . 15

4. Shape Factor H, $Re_{\delta}^*/\sqrt{Re_L}$ and $Re_{\theta}/\sqrt{Re_L}$ for Final Body Shape . . . 16

5. Pressure Gradient Parameter λ for Final Body Shape . . . 16

6. Stability Roots σ_n versus Vehicle Speed . . . 28

7. $Re_{\delta}^*/\sqrt{Re_L}$ and the Quantity 2900 exp $(0.08\Lambda)/\sqrt{Re_L}$ for Vehicle Speeds of 1 to 5 Knots . . . 31

8. Thrust Coefficient K_T and Propeller Efficiency η_p versus Advance Ratio J, 3 Blade BAR = .58 p/d = 1.41 . . . 39

9. Torque Coefficient K_Q versus Advance Ratio J, 3 blade BAR = .58, p/d = 1.41 . . . 39

10. Motor RPM, Power Output HP, Current Draw I and Efficiency η_m versus Torque Q motor type Minnesota Electric Technology Inc., C32-BB-2, 24 VDC . . . 42

TABLES

1. NOSC Shape Characteristics . . . page 12

2. Transition Location . . . 31

3. Laminar Flow Length Allowance . . . 32

4. Skin Friction Coefficient . . . 32

5. Afterbody Drag Coefficient . . . 33

6. Fin Drag Coefficients . . . 34

7. Nozzle Drag Coefficient . . . 35

8. Hull Induced Drag Coefficient . . . 36

9. Drag Contribution of Individual Components . . . 37

NOMENCLATURE

A	σ^3 coefficient of Equation 13, also laminar flow length allowance Equation 51 Section 4
A_f	planform area of fin(s)
AR	fin aspect ratio ($span^2/A_f$)
A_w	wetted surface area
B	σ^2 coefficient of Equation 13
b	fin semi-span
C	σ^1 coefficient of Equation 13
C_{Di}	induced drag body lift coefficient
C_{D_o}	drag coefficient based on frontal area
C_f	skin friction coefficient
C_L	body lift coefficient
C_{Lf}	fin lift coefficient
C_p	prismatic coefficient Equation 2
D	maximum body diameter
d	propeller diameter
D_1	σ^o coefficient of Equation 13

f	body fineness ratio
F_1	PGG polynomial Equation 1c
F_2	PGG polynomial Equation 1d
F_B	net buoyancy force
G	PGG polynomial Equation 1e
g	acceleration of gravity
H	boundary layer shape factor, δ^*/θ
HP	motor horsepower
I	motor current
I_o	moment of inertia (about y axis) of displaced water
I_y	vehicle moment of inertia about y axis
I'_y	dimensionless moment of inertia
J	propeller advance ratio Equation 59
k'	coefficient of accession (ellipsoid of revolution)
K_1	body curvature at X_m Equation 1i
k_1	dimensionless body curvature at X_m Equation 1g also coefficient of accession Section 3
k_2	coefficient of accession (ellipsoid of revolution)

K_Q	propeller torque coefficient Equation 58
K_T	propeller thrust coefficient Equation 57
K_{TP}	thrust
L	overall body length
M	moment around y (pitch) axis
m	mass of vehicle
M'	dimensionless moment around y axis
m'	dimensionless mass of vehicle
n	propeller shaft speed
p	propeller pitch
Q	propeller torque
R	body radius
Re_L	length Reynolds number $(U_\infty L/\nu)$
Re_x	$U_\infty x/\nu = Re_L(x/L)$
Re_{xtr}	Re_x at boundary layer transition
$Re_{\delta*}$	displacement thickness Reynolds number $(U_e \delta*/\nu)$
$Re_{\delta*_{tr}}$	$Re_{\delta*}$ at boundary layer transition
Re_θ	momentum thickness Reynolds number $(U_e \theta/\nu)$

R_h	radius of curvature at nose Equation 1h
r_n	dimensionless nose radius Equation 1f
s	surface arc length
T	propeller thrust
t	time (also thrust deduction Section 5)
u	boundary layer velocity (function of y)
U_a	propeller speed of advance
U_e	local velocity at boundary layer edge
U_∞	freestream velocity (also vehicle speed)
w	wake fraction factor Equation 61
w_t	trailing edge angle (Bottaccini)
x	axial distance
x	nondimensional axial distance also axial distance for Section 3
$\bar{x}$	see Equation 35
x_o	see Equation 35
x_B	axial location of center of pressure (hull only)
x_{cB}	axial location of centroid of volume
x_f	axial location of center of pressure of fin

X_m	axial distance from nose to cylindrical intersection
y	boundary layer coordinate normal to surface, also horizontal axis in Section 3
Z	force in z direction
z	vertical axis in Section 3
Z'	dimensionless force in z direction
z_m	metacentric distance
α	angle of attack of body
$\dot{\alpha}$	$d\alpha/dt$, rate of change of α
β	propeller canting angle
γ	fin sweepback angle
δ^*	boundary layer displacement thickness Equation 7
δ_s	stern plane deflection angle
η_m	motor efficiency Equation 66
η_p	propeller efficiency
θ	boundary layer momentum thickness Equation 8, Section 2, also angle from horizontal earth axis in Section 3
$\dot{\theta}$	$d\theta/dt$ notational velocity Section 3
$\ddot{\theta}$	$d^2\theta/dt^2$ angular acceleration Section 3

Λ Pohlhausen pressure gradient parameter

λ pressure gradient parameter Equation 5

ν kinematic viscosity

ρ water density

σ_i $i = 1,2,3$ stability equation roots, Equation 13

Superscripts used in Section 3

' denotes dimensionless quantity

Subscripts used in Section 3

$\alpha, \dot{\alpha}$ denotes partial differential with respect to α or $\dot{\alpha}$

$\theta, \dot{\theta}, \ddot{\theta}$ denotes partial differentiation with respect to θ, $\dot{\theta}$, $\ddot{\theta}$

f references to fins only

h references to body hull only

SECTION 1

INTRODUCTION

The development of the NOSC Free-Swimming Submersible has been undergoing development at NOSC for several years. Basically the Free-Swimming Submersible is designed to be an untethered, unmanned submersible capable of performing preprogrammed maneuvers without operator control. Heckman[1] gives a full description of the vehicle design and performance as presently configured. Figure 1, taken from Heckman, shows the vehicle in its present (1982) configuration. Figure 2 shows the vehicle in the planned configuration.

This vehicle is propelled by two motor-thruster units, rated at 1/4 HP each, mounted at the rear of the vehicle. Propellers (7.5 inches diameter) mounted in nozzles provide thrust. The thruster units are canted 15° from the vehicle centerline; directional control in the horizontal plane is achieved by varying the thrust from each unit. This method allows turns to be made at near zero forward speed. A third thruster, mounted vertically near the center of the vehicle provides depth control. At present, the vehicle components (frame, cameras, battery cannisters, etc.) are all exposed to water flow, giving the vehicle a large drag coefficient which limits top speed to about 1.8 knots.

To increase endurance at low speeds and increase top speed to about 5 knots, Code 9411 has designed a compact frame to enable the major components of the submersible to be enclosed by a low drag fairing. This report describes the hydrodynamic design assistance provided by NOSC Code 6342, the Fluid Mechanics and Materials Branch, in the design of that fairing.

---

1. Heckman, Paul J., Jr., Free-Swimming Submersible Testbed (EAVE WEST), Naval Ocean Systems Center TR 622, September 1980.

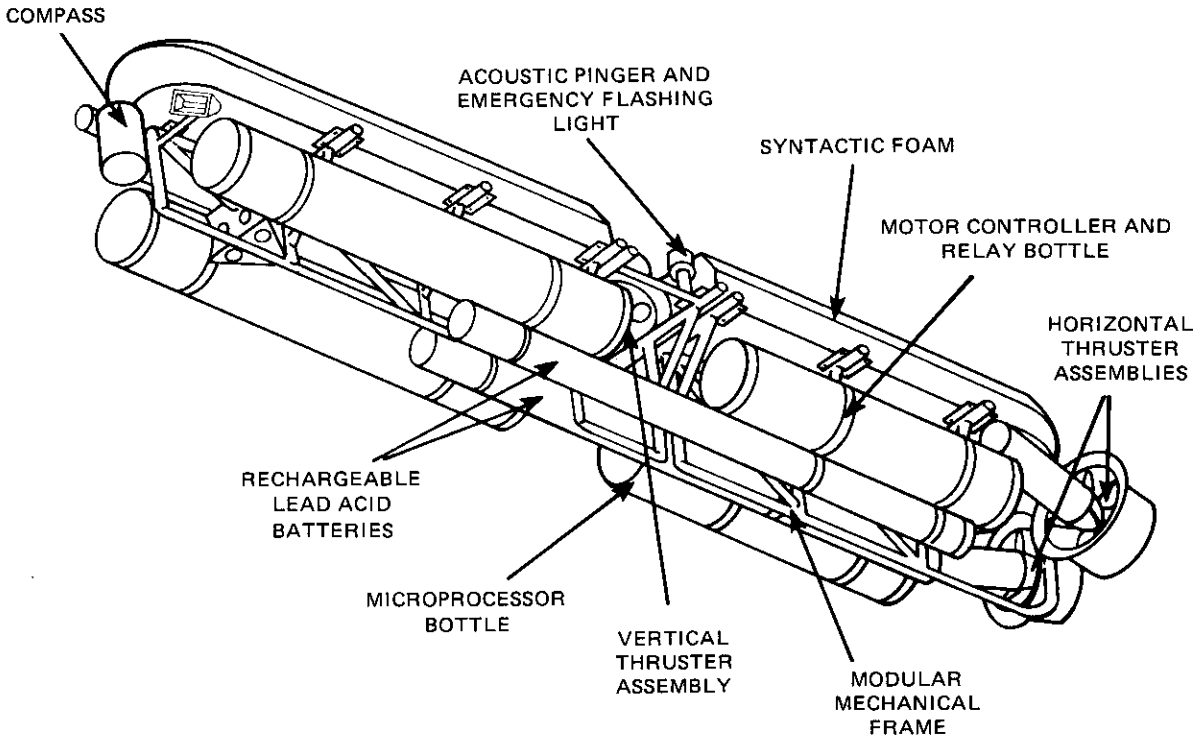

Figure 1. NOSC free-swimming vehicle concept, testbed configuration.

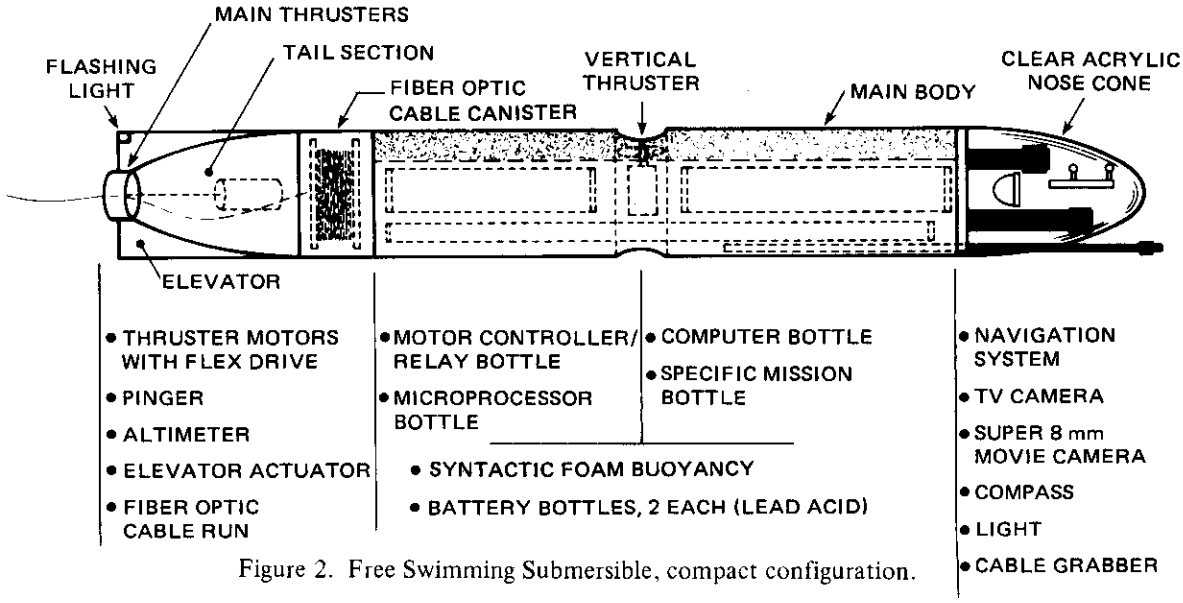

Figure 2. Free Swimming Submersible, compact configuration.

SECTION 2

NOSE AND TAIL SHAPE

To facilitate the installation of optical instruments (TV cameras, etc.), the nose portion of the fairing is to be manufactured from clear acrylic. The fairing portion of the vehicle is free-flooded, hence depth pressure forces on the nose are minimal. Since the speed of the vehicle is relatively slow, low drag laminar boundary layer flow can be maintained over a major portion of the forebody with a suitably designed nose. The major hydrodynamic design constraint is that the nose must fair in smoothly with a cylindrical midsection 19 inches in diameter. This type of nose configuration always results in a local flow deceleration (adverse pressure gradient) near the nose-cylinder point of tangency. Too strong an adverse pressure gradient will cause laminar flow separation and subsequent transition to turbulent flow. For the same flow conditions, a turbulent boundary layer flow has about seven times greater skin friction than laminar flow; therefore, it obviously is desirable to maintain as much laminar flow as possible.

Laminar boundary layer calculations were performed for 10 different nose shapes (characteristics shown in Table 1). The noses labeled PGG in Table 1 are described by an analytical expression for noseshape developed by Parsons, Goodson and Goldschmied[2]. This expression is

$$R(X)/L = 1/(2f)[r_h F_1(x) + k_1 F_2(x) + G(x)]^{1/2} \tag{1a}$$

where $0 \leq X \leq X_m$

and

$$x = X/X_m \tag{1b}$$

$$F_1(x) = -2x(x-1)^3 \tag{1c}$$

---

2. Parsons, J. S., Goodson, R. E. and Goldschmied, F. R., Shaping of Axisymmetric Bodies for Minimum Drag in Incompressible Flow, J. of Hydronautics Vol. 8, No. 3, July 1974, pp. 100-107.

No.	Description (equation)	Radius, R_n $x = 0$	NOSE Length, X_m	Comments
1	Hemisphere	R_{max}	R_{max}	severe separation
2	2:1 Ellipse	$(1/2)R_{max}$	$2R_{max}$	separation
3	4:1 Ellipse	$(1/4)R_{max}$	$4R_{max}$	no separation, but extremely long nose
4	PGG	$(2/7)R_{max}$	$3R_{max}$	near separation $H_{max}=3.3$
5	PGG	R_{max}	$2R_{max}$	separation
6	PGG	$(4/7)R_{max}$	$3R_{max}$	good $H_{max}=2.99$
7	PGG	$(6/7)R_{max}$	$3R_{max}$	separation
8	PGG	$(4/7)R_{max}$	$2.5R_{max}$	near separation $H_{max}=3.4$
9	PGG	$(3/7)R_{max}$	$3R_{max}$	fair $H_{max}=3.1$
10	PGG	$(1/2)R_{max}$	$3R_{max}$	good $H_{max}=3.01$

Table 1. NOSC shape characteristics.

$$F_2(x) = -x^2(x-1)^2 \tag{1d}$$

$$G(x) = x^2(3x^2-8x+6) \tag{1e}$$

$$r_n = (4X_m/D^2)Rn \tag{1f}$$

$$k_1 = (-2X_m^2/D)K_1 \tag{1g}$$

$$R_n = \text{radius of curvature at nose} \tag{1h}$$

$$= 1/(d^2X/dR^2) \text{ at } X=0$$

$$K_1 = \text{body curvature at } X_m \tag{1i}$$

$$= d^2R(X_m)/dX^2$$

$$f = \text{fineness ratio} = L/D \quad . \tag{1j}$$

In Equation 1, L is the total vehicle length, R is body radius, D(=2R max) is body maximum diameter and X_m is the axial distance from the nose to the point of cylindrical tangency.

Boundary layer parameters were calculated using a Thwaites integral solution for laminar flow adapted from Cebeci and Bradshaw[3], programmed on the NOSC UNIVAC 1100/82 computer in FORTRAN. Three computer programs were required to complete a test case for each nose (body) shape. Program COORD is required to calculate and format the body offset and control cards for input into the axisymmetric potential flow program (HODAPF) developed by McDonnell Douglas Corporation (Friedman[4]). The output of HODAPF is the potential flow

---

3. Cebeci, T. and Bradshaw, P., Momentum Transfer in Boundary Layers, McGraw-Hill, 1977, pg. 108.

4. Friedman, D. M., Improved Solution for Potential Flow about Arbitrary Axisymmetric Bodies by the use of a Higher Order Surface Source Method Part II, User's Manual for Computer Program, NASA CR 134695, July 1974.

velocity (or pressure coefficient) as a function of axial position required for input into program LAMINR which calculates and plots the boundary layer parameters. Both program COORD and LAMINR require a function subroutine called RVSX which contains the equation(s) which describe the body shape. Appendix A shows the program listings and a sample run.

Figure 3 shows the potential flow velocity ratio (U_e/U_∞) as a function of axial position (X/L) for a body with a PGG nose (No. 6 in Table 1), cylindrical center section and a 2:1 circular arc tail. The quantity U_∞ is the freestream velocity (or forward speed) and U_e is the local velocity at the edge of the boundary layer. Figures 4 and 5 show the calculated boundary layer parameters for this body. Calculations were stopped at X/L = 0.6 since disturbances caused by the presence of the vertical thruster at about X/L = 0.5 would preclude any further laminar flow. The dimensionless parameters in Figures 3 and 4 are defined as:

$$Re_L = \text{length Reynolds no.} = \frac{U_\infty L}{\nu} \tag{2}$$

$$Re_{\delta^*} = \text{displacement thickness Reynolds no.} = \frac{U_e \delta^*}{\nu} \tag{3}$$

$$Re_\theta = \text{momentum thickness Reynolds no.} = \frac{U_e \theta}{\nu} \tag{4}$$

$$\lambda = \frac{\theta^2}{\nu} \frac{dU_e}{ds} \tag{5}$$

$$H = \text{shape factor} = \frac{\delta^*}{\theta} \tag{6}$$

$$\delta^* = \text{displacement thickness} = \int_0^\infty (1 - u/U_e)dy \tag{7}$$

$$\theta = \text{momentum thickness} = \int_0^\infty (u/U_e)\ (1-u/U_e)dy \tag{8}$$

where ν is the fluid kinematic viscosity, s is the surface arc length distance from the nose, y is the distance normal to the vehicle surface and u is the

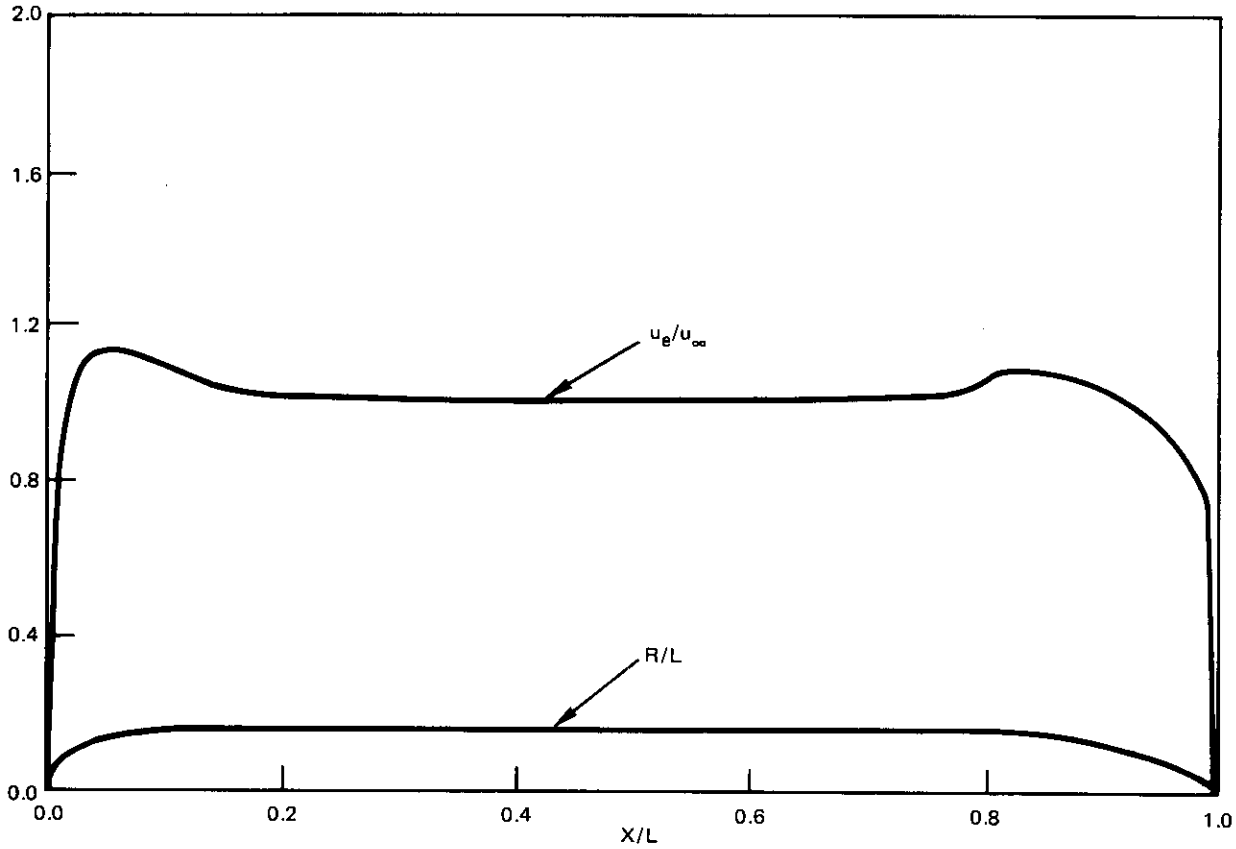

Figure 3. Potential flow and body radius versus X/L, for final body shape.

local boundary layer velocity (a function of y). The particular method of presentation in Figures 3 and 4, make the laminar boundary layer calculations independent of both vehicle speed and size, such that body shape becomes the only independent variable, and thus can be easily evaluated.

The criterion used to predict laminar separation for this study was that separation occurs if the pressure gradient parameter is less than -0.09 (White[5]). This corresponds to a maximum boundary layer shape factor, H of 3.55. A summary of the calculated results for ten nose shapes (one hemispherical, two elliptical and seven PGG noses) is presented in Table 1. The nose shape with the best resistance to laminar separation (No. 6 in Table 1) is a PGG nose which has a nose radius, R_n of 4/7 R_{max} and a nose length, X_m of 3 R_{max} (smooth intersection with a cylindrical midbody implies that K_1 (Equation 1i) is equal to zero). For this nose the maximum shape factor H is 2.99

5. White, F. M., Viscous Fluid Flow, McGraw-Hill, 1974, pg. 432 (Eq 5-39), pg. 316.

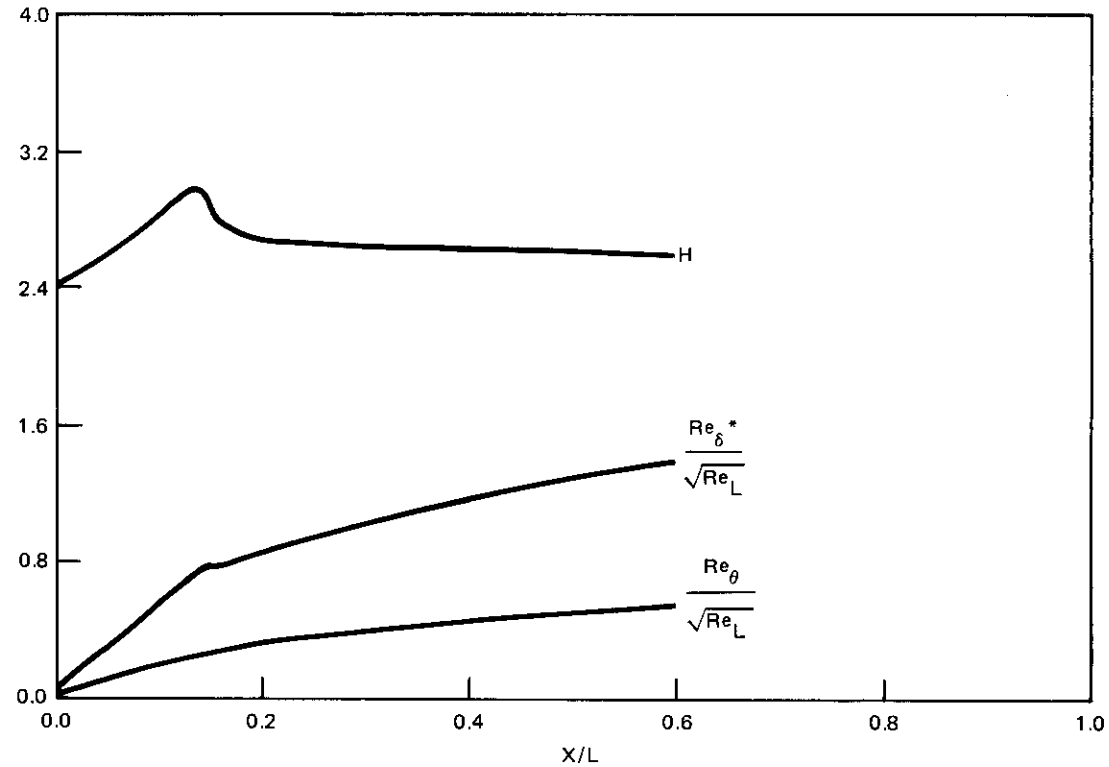

Figure 4. Shape factor H, $Re_\delta{}^*/\sqrt{Re_L}$ and $Re_\theta/\sqrt{Re_L}$ for final body shape.

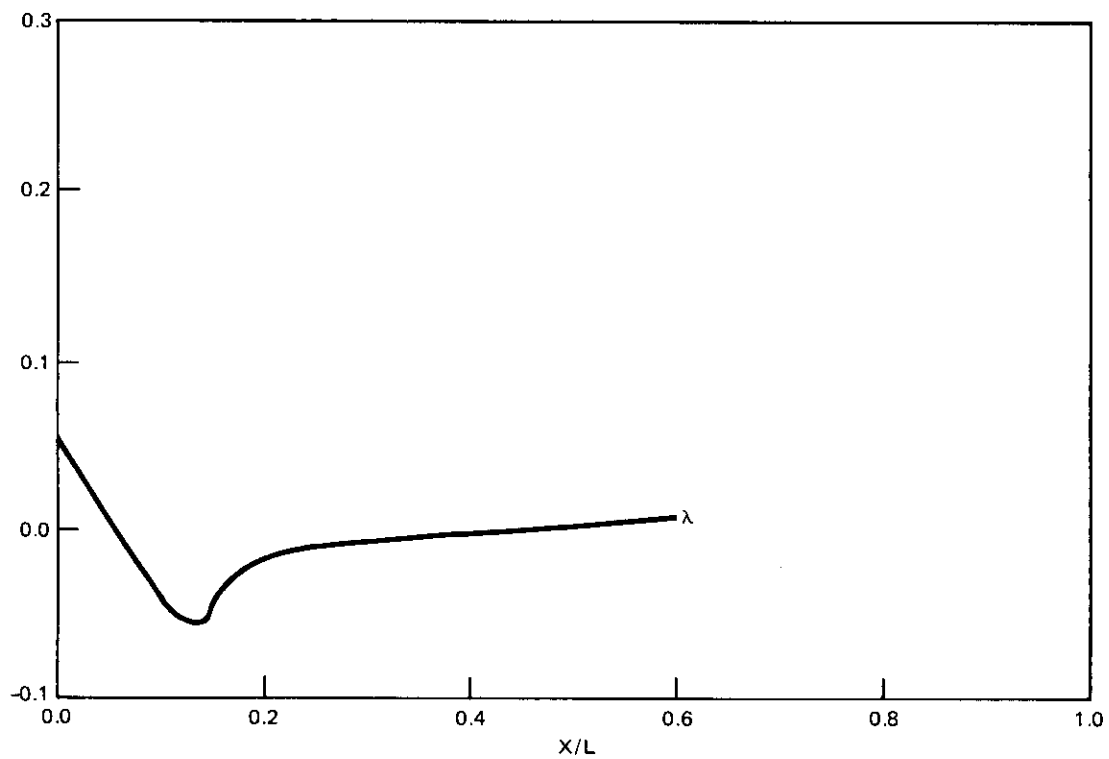

Figure 5. Pressure gradient parameter λ for final body shape.

and the minimum pressure gradient parameter λ is -0.058. This nose shape is used on the final fairing design, where R_{max} = 9.5 in. (241.3 mm), R_n = 5.429 in.(137.9 mm) and X_m = 28.5 in. (723.9 mm).

For vehicle speeds above about one knot with the disturbances caused by the vertical thruster and/or other appendages, turbulent boundary layer flow will be well developed by the afterbody of the vehicle. This is desirable since turbulent flow is resistant to flow separation. Flow separation on the afterbody would cause an area of low pressure to exist which, depending on its extent, can be the major component of drag of the vehicle. The optimum shape of the afterbody is a compromise between minimizing the surface area (minimal frictional drag) and gently fairing the tail to minimize flow separation (minimal pressure drag). Hoerner[6] presents a graph of the experimentally determined afterbody drag as a function of the length of the tail, when added to a cylindrical shape. Both rounded and pointed tail shapes were considered, with the rounded tail having only a slightly lower drag coefficient. The minimum drag occurred for a tail length/diameter ratio of 2.0. For smooth shapes with turbulent boundary layer flow, the actual contour of the afterbody appears to be relatively unimportant as long as flow separation is avoided. For this reason a simple circular arc contour with a length/diameter ratio of 2.0 was chosen for the shape of the afterbody. For a body diameter of 19 in. (482.6 mm) the length of the afterbody becomes 38 in. (965.2 mm) with a constant radius of curvature of about 81 in. (2057 mm) and a tail intersection half angle of 28°.

---

6. Hoerner, Sighard F., Fluid-Dynamic Drag, Published by the author, 1965, pg. 20-2, pg. 3-12, pg. 8-12, pg. 7-17.

SECTION 3

VEHICLE STABILITY

The term "controls fixed stability" means that any perturbation from the mean motion will eventually damp out, without any action from active control surfaces. For a submersible with a vertical separation (metacentric distance) between the center of buoyancy and center of gravity, controls fixed stability in the vertical (pitch) plane implies that the vehicle will return to a path of constant depth after a disturbance. Stability in the horizontal (yaw) plane implies that the vehicle will return to a constant heading after a disturbance. For very slow speed submersibles, pitch stability can be provided solely by the metacentric restoring moment. However, for higher speeds, hydrodynamic forces (proportional to velocity squared) quickly dominate and some sort of hydrodynamic stabilizers (fins) are required. For a much more complete explanation of vehicle stability see Arentzen and Mandel[7] and/or Comstock[8].

Nomenclature for this section is as follows: the x axis is defined to be parallel to the axis of the vehicle, the y axis is perpendicular to the vehicle axis in the horizontal plane and the z axis is perpendicular to the vehicle axis in the vertical plane. Possible motions of a vehicle are the translations in the x, y and z direction plus the rotations around each axis designated roll, pitch and yaw which are rotations around the x, y and z axes, respectively. Considering only pitch stability for the moment, the following definitions apply: the angle of attack α is measured from the resultant velocity vector U_∞ to the x axis of the submersible, the angular position from the horizontal earth axis to the x-axis of hull is designated θ. Angular velocities about the y-axis are designated $\dot{\theta}$ and $\dot{\alpha}$ (dots represent derivatives with respect to time) and angular acceleration is designated $\ddot{\theta}$.

---

7. Arentzen, E. S. and Mandel, P., Naval Architectural Aspects of Submarine Design, Trans SNAME, 1960.

8. Comstock, J. P., ed. Principles of Naval Architecture, SNAME 1967, Chapter VIII.

Using the shorthand notation common to naval architectural work, the forces on a submersible in the z direction are designated Z and the moments around the pitch axis (y-axis) are designated M. Partial derivatives are designated with subscripts (i.e., $M_\alpha = \frac{\partial M}{\partial \alpha}$) and dimensionless terms are designated with primes. From Arentzen and Mandel[7] the nondimensionalized force equation in the z direction is

$$(Z'_{\dot{\alpha}} - m')\dot{\alpha} + Z'_\alpha \alpha + (Z'_{\dot{\theta}} + m')\dot{\theta} + Z'_{\delta_s} \delta_s = 0 \tag{9}$$

and the moment equation around the y axis is

$$(M'_{\ddot{\theta}} - I'_y)\ddot{\theta} + M'_\alpha \alpha + M'_{\dot{\theta}} \dot{\theta} + M'_\theta \theta + M'_{\delta_s} \delta_s = 0 \quad , \tag{10}$$

where δ_s is the stern plane deflection angle, m' is the nondimensional mass, $m/(\rho/2)L^3$, I'_y is the nondimensional mass moment of inertia about the y-axis, $I_y/(\rho/2)L^5$, ρ is fluid density and L is vehicle length. With controls fixed, the terms $Z'_{\delta_s}\delta_s$ and $M'_{\delta_s}\delta_s$ are constants and Equations 9 and 10 combine into a third order differential equation with solutions of the form

$$\alpha = \alpha_1 \exp(\sigma_1 t) + \alpha_2 \exp(\sigma_2 t) + \alpha_3 \exp(\sigma_3 t) \tag{11}$$

$$\theta = \theta_1 \exp(\sigma_1 t) + \theta_2 \exp(\sigma_2 t) + \theta_3 \exp(\sigma_3 t) \tag{12}$$

where α_n and θ_n are constants of integration, σ_1, σ_2 and σ_3 are the stability indices with dimensions of 1/time and t is time. It can be seen from Equations 11 and 12 that if any real portion of σ is positive, α and θ will increase with time and the motion is unstable. Imaginary values of σ imply an oscillatory motion. Only if all real values of σ are negative will α and θ decrease with time, indicating stable motion.

Substitution of Equations 11 and 12 into Equations 9 and 10 produce the following characteristic equation in σ

$$A\sigma^3 + B\sigma^2 + C\sigma + D_1 = 0 \tag{13}$$

where

$$A = (M'_{\ddot{\theta}} - I'_y)\ (Z'_{\dot{\alpha}} - m') \tag{14a}$$

$$B = (M'_{\ddot{\theta}} - I'_y)Z'_\alpha + (Z'_{\dot{\alpha}} - m')M'_{\dot{\theta}} \tag{14b}$$

$$C = Z'_\alpha\ M'_{\dot{\theta}} - (Z'_{\dot{\theta}} + m')M'_\alpha + (Z'_{\dot{\alpha}} - m')M'_\theta \tag{14c}$$

$$D_1 = Z'_\alpha\ M'_\theta \quad . \tag{14d}$$

The question of vehicle stability reduces to evaluating the coefficients A, B, C and D_1, and solving for the roots σ_1, σ_2 and σ_3 of Equation 13.

Evaluation of the coefficients of Equation 13 is complex due to the large number of force and moment derivatives involved. The equations used for calculation of these derivatives will be presented here, with little comment as to the theory of their derivation. The reader is referred to Comstock and Bottaccini[9] for a more complete explanation. In the following equations the subscript h refers to the derivative for the hull only and the subscript f refers to the appropriate derivative for the fins. Continuing

$$I'_y = \frac{I_y}{(\rho/2)L^5} \tag{15}$$

$$m' = \frac{m}{(\rho/2)L^3} \tag{16}$$

---

9. Bottaccini, M. R., The Stability Coefficients of Standard Torpedoes, NAVORD Rept. 3346, 1954.

where I_y and m are the moment of inertia and mass of the vehicle including any entrained water when submerged. The metacentric moment derivative is (for small perturbations and θ in radians)

$$M_\theta = \frac{\partial M}{\partial \theta} = -m_a g z_m \tag{17}$$

where g is the acceleration of gravity, z_m is the metacentric distance and m_a is the in-air mass of the vehicle (assuming z_m is evaluated not including entrained water). Also

$$M'_\theta = \frac{M_\theta}{(\rho/2)L^3 U_\infty^2} \quad . \tag{18}$$

From Bottaccini[9], the angle of attack moment derivative for the hull is

$$\begin{aligned} M_\alpha\Big)_h = (\rho/2)U_\infty^2 L(\pi/4)D^2 \Big[& 2C_p(k_2-k_1) \\ & -(x_B/L)(0.005f^2 + 0.96C_p + 5.71\ |0.833 - C_p| \\ & - 0.012\ w_t)\Big] \end{aligned} \tag{19}$$

where

$$X_B = (L - X_{CB})(1. - .0111w_t)\ 0.78 \tag{20}$$

$$C_p = \text{prismatic coefficient} = \frac{\text{displaced volume}}{(\pi/4)D^2 L} \quad . \tag{21}$$

k_1 and k_2 are the theoretical hydrodynamic accession coefficients for ellipsoids with fineness ratio f. Also, in Equation 20 X_{CB} is the distance from the nose to the centroid of the vehicle volume and w_t is a trailing-edge angle as defined in Bottaccini. This moment derivative is destabilizing $(M_\alpha)_h>0$);

an angle of attack α produces a moment which tends to increase α. From Comstock the moment derivative for the fins is

$$M_\alpha\Big)_f = -x_f(\rho/2)U_\infty^2 \quad A_f \frac{\partial C_{Lf}}{\partial \alpha} \tag{22}$$

where A_f is the fin area, x_f is the location (from X_{CB}) of the fin center of pressure and the fin lift coefficient slope ($\partial C_{Lf}/\partial\alpha$) is

$$\frac{\partial C_{Lf}}{\partial \alpha} = \frac{0.9\ (2\pi)\ AR}{\left(\cos\ \gamma\left(\frac{AR^2}{\cos^4\gamma} + 4\right)^{0.5}\right) + 1.8} \quad . \tag{23}$$

In Equation 23 AR is the fin aspect ratio (= span^2/A_f) and γ is the fin sweepback angle. Then

$$M_\alpha = M_\alpha\Big)_h + M_\alpha\Big)_f \tag{24}$$

and

$$M'_\alpha = \frac{M_\alpha}{(\rho/2)L^2U_\infty^2} \quad . \tag{25}$$

A vehicle with large fins where the overturning moment of the hull is completely balanced by the fins (i.e., $M_\alpha<0$) is called statically stable. Generally, most vehicles (i.e., ships, torpedoes, etc.) are not statically stable, but are dynamically stable due to the influence of dynamic forces which counteract the hull moment. Static stability is not necessarily desirable, since large fins are required and turning rates may be slow.

The angle of attack side force derivatives are similar to the moment derivatives, thus, from Bottaccini

$$Z_\alpha\Big)_h = -(\rho/2)(\pi/4)D^2U_\infty^2\,[0.005f^2 + 0.96C_p$$

$$+ 5.71\,|.835 - C_p| - 0.012w_t] \tag{26}$$

and from Comstock

$$Z_\alpha\Big)_f = -(\rho/2)U_\infty^2 A_f \frac{\partial C_{Lf}}{\partial \alpha} \tag{27}$$

then

$$Z_\alpha = Z_\alpha\Big)_h + Z_\alpha\Big)_f \tag{28}$$

and

$$Z'_\alpha = \frac{Z_\alpha}{(\rho/2)L^2U_\infty^2} \quad . \tag{29}$$

From Comstock the rotary side force derivatives are

$$Z'_\theta\Big)_h = -k_1 m' + \frac{x_B}{L} Z'_\alpha\Big)_h \tag{30}$$

and

$$Z'_\theta\Big)_f = \frac{x_f}{L} Z'_\alpha\Big)_f \tag{31}$$

where

$$Z'_\alpha\Big)_h = \frac{Z_\alpha\Big)_h}{(\rho/2)L^2U_\infty^2} \tag{32}$$

and

$$Z'_{\alpha}\Big)_f = \frac{Z_{\alpha}\Big)_f}{(\rho/2)L^2U_{\infty}^2} \tag{33}$$

then

$$Z'_{\dot{\theta}} = Z'_{\dot{\theta}}\Big)_h + Z'_{\dot{\theta}}\Big)_f \quad . \tag{34}$$

The rotary moment derivatives are

$$M'_{\dot{\theta}}\Big)_h = -m'_z \frac{\bar{x}}{L} + \left(\frac{x_0}{L}\right)^2 Z'_{\alpha}\Big)_h \tag{35}$$

and

$$M'_{\dot{\theta}}\Big)_f = \left(\frac{x_f}{L}\right)^2 Z'_{\alpha}\Big)_f \quad . \tag{36}$$

The quantity $\bar{x}$ involves a complex integration procedure and is usually very small, so for this study it was assumed to be zero. From Comstock the quantity x_0/L is approximately equal to $C_p/2$, then

$$M'_{\dot{\theta}}\Big)_h = \left(\frac{C_p}{2}\right)^2 Z'_{\alpha}\Big)_h \tag{37}$$

and

$$M'_{\dot{\theta}} = M'_{\dot{\theta}}\Big)_h + M'_{\dot{\theta}}\Big)_f \quad . \tag{38}$$

Also from Comstock

$$Z_{\dot{\alpha}}\Big)_h = -k_2 U_\infty (\text{displaced mass}) = -k_2 U_\infty C_p \rho (\pi/4) L D^2 \tag{39}$$

and

$$Z_{\dot{\alpha}}\Big)_f = -\frac{\pi \rho b A_f U_\infty}{((AR)^2 + 1)^{0.5}} \tag{40}$$

where b is the fin semispan and the other terms have been defined previously. Then

$$Z_{\dot{\alpha}} = Z_{\dot{\alpha}}\Big)_h + Z_{\dot{\alpha}}\Big)_f \tag{41}$$

and

$$Z'_{\dot{\alpha}} = \frac{Z_{\dot{\alpha}}}{(\rho/2) L^3 U_\infty} \quad . \tag{42}$$

For near elliptical bodies, the acceleration moment derivative for the hull is

$$M_{\ddot{\theta}}\Big)_h \simeq -k' I_0 \quad , \tag{43}$$

where k' is the Lamb coefficient for accession to inertia in rotation (for ellipsoids of fineness ratio f) and I_0 is the moment of inertia of the displaced water. For an ellipsoid

$$I_0 = (\text{displaced mass}) \left[\frac{\left(\frac{L}{2}\right)^2 + \left(\frac{D}{2}\right)^2}{5}\right] \quad , \tag{44}$$

then for an arbitrary slender body

$$I_0 \simeq c_p \, L^3 \, (\pi/4) \, D^2 \rho \left[\frac{1 + (1/f)^2}{20}\right] \tag{45}$$

for the fins

$$0 \simeq M_{\ddot{\theta}}\Big)_f << M_{\ddot{\theta}}\Big)_h \tag{46}$$

then

$$M'_{\ddot{\theta}} \simeq \frac{M_{\ddot{\theta}}\Big)_h}{(\rho/2)\ L^5} \quad . \tag{47}$$

With Equations 15 through 47 the coefficients of Equation 14 can be evaluated and Equation 13 solved for the stability indices.

Equations 13 and 14 are the equations of motion in the vertical plane. The equations of motion in the horizontal plane are very similar to Equation 13 except that the term M'_θ is zero (there is no metacentric moment in the horizontal plane). This reduces Equation 13 to a second order differential equation and, of course, the various motion derivatives now apply to the vertical fins or control surfaces rather than the horizontal fins. The stability indices in the vertical plane are speed dependent while the stability indices in the horizontal plane are not, since the term M'_θ varies with speed. At very large speeds, $M'_\theta \to 0$ and the equations of motion in the vertical plane became the same as the horizontal plane.

The FORTRAN program COEFF was developed on the NOSC UNIVAC 1100/82 to calculate the various motion derivatives and the roots of the characteristic equation (Equation 13), given the geometric characteristics of the vehicle. For the fairing and tail fin design of Figure 5, the following characteristics apply:

L = 15.5 ft (4.724 m)

D = 1.583 ft (0.483 m)

C_p = 0.8715

$w_t = 76.2°$

$x_f = 7.111$ ft (2.167 m)

$A_f = 1.667$ ft^2 (0.155 m^2)

$AR = 1.504$

$\gamma = 0.°$

$b = 0.792$ ft (0.241 m)

$X_{cB} = 7.31$ ft (2.228 m) .

For sea water at 40°F

$\rho = 1.9933$ slugs/ft^3 (1028 kg/m^3).

From Comstock for L/D = f = 9.792

$k_1 = 0.03 \quad k_2 = 0.96 \quad k' = 0.88$.

The in-air mass of the vehicle was estimated to be about 660 lbs with a metacentric distance of 0.5 ft or

$m = 20.497$ slugs (299.4 kg)

$z_m = 0.5$ ft (.152 m) .

The mass of the vehicle including entrained water was approximated by assuming that the volume enclosed by the fairing is neutrally buoyant as was the body moment of inertia with the additional assumption that the mass was uniformly distributed. Then

$m = 52.86$ slugs (772 kg)

$I_y = I_0 = 829.6$ slugs ft^2 (1125 kg - m^2) .

Figure 6 shows the calculated stability roots as a function of speed for the vehicle with the above physical characteristics. The roots σ_1 and σ_3 are complex conjugates with a negative real part as shown in Figure 6. The root σ_2 is real and less than zero through the speed range. Negative values for the real parts of σ_1, σ_2 and σ_3 indicate that this vehicle is dynamically stable in pitch. Stability in the yaw plane was checked by setting M_θ equal to zero and assuming that the hydrodynamic characteristics of the vertical fins are essentially the same as the horizontal fins. For this case $\sigma_1 = -0.1693$ sec^{-1} and $\sigma_2 = -2.663$ sec^{-1} ($\sigma_3 = 0$ since Equation 13 becomes second order for $M_\theta = 0$) and are independent of speed. Thus, the vehicle is also stable in the yaw plane.

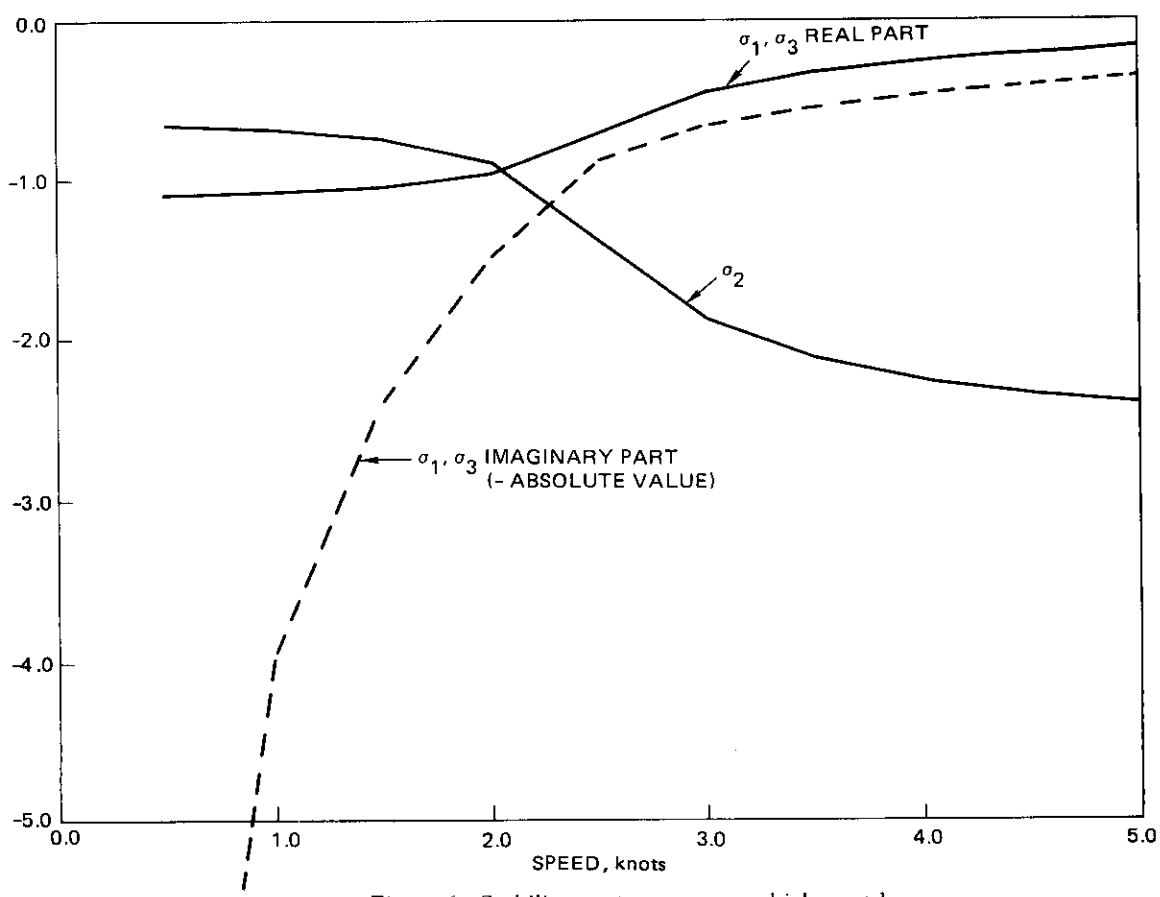

Figure 6. Stability roots σ_n versus vehicle speed.

The calculated nondimensional moment derivative (independent of speed) for this hull is

$$M'_\alpha\Big)_h = 13.05 \times 10^{-3}$$

and the nondimensional moment derivative for the fins is

$$M'_\alpha\Big)_f = -6.29 \times 10^{-3} \quad .$$

Since the quantity M'_α $(= M'_\alpha\Big)_h + M'_\alpha\Big)_f)$ is greater than zero, this vehicle is <u>not</u> statically stable.

As a simple check of the margin of stability of this vehicle, stability roots were calculated for cases with smaller fin plan areas (everything else is the same). For these cases, pitch stability (at 5 knots) disappeared at a fin area of 0.73 A_f and yaw stability disappeared at a fin area of 0.88 A_f. Yaw stability appears to be only marginal considering the number of assumptions involved in the stability calculations. However, the stabilizing effect of the propeller nozzles was not included in the calculations for yaw stability, so it is felt that the stability margin in this plane is adequate.

SECTION 4

VEHICLE DRAG

A strong influence on total vehicle drag is the location of laminar to turbulent boundary layer transition. White[5] presents a very simplified criterion for transition with an experimentally determined correlation

$$Re_{\delta^*_{tr}} = 2900\ e^{0.08\Lambda} \tag{48}$$

where $Re_{\delta^*_{tr}}$ is the displacement thickness and Reynolds number at transition and Λ is the Pohlhausen pressure gradient parameter. The Pohlhausen pressure gradient parameter is related to the parameter λ (Equation 5 of Section 2) by the relation

$$\lambda = \Lambda \left(\frac{37 - \Lambda/3 - 5\Lambda^2/144}{315} \right)^2 \quad . \tag{49}$$

The calculated curve of $Re_{\delta^*}/\sqrt{Re_L}$ of Figure 3 can be used to determine the approximate location of transition. The criterion is that the flow becomes turbulent when

$$\frac{Re_{\delta^*}}{Re_L} > \frac{2900\ e^{0.08\Lambda}}{\sqrt{Re_L}} \quad . \tag{50}$$

Figure 7 shows curves of the quantity $Re_{\delta^*}/\sqrt{Re_L}$ and the quantity 2900 $\exp(0.08\Lambda)/\sqrt{Re_L}$ (from Section 2) versus X/L for vehicle speeds of 1,2,3,4 and 5 knots (seawater at 40°F). Using Equation 50 or assuming that laminar flow cannot exist past X/L = 0.5 results in transition locations versus vehicle speed as listed in Table 2.

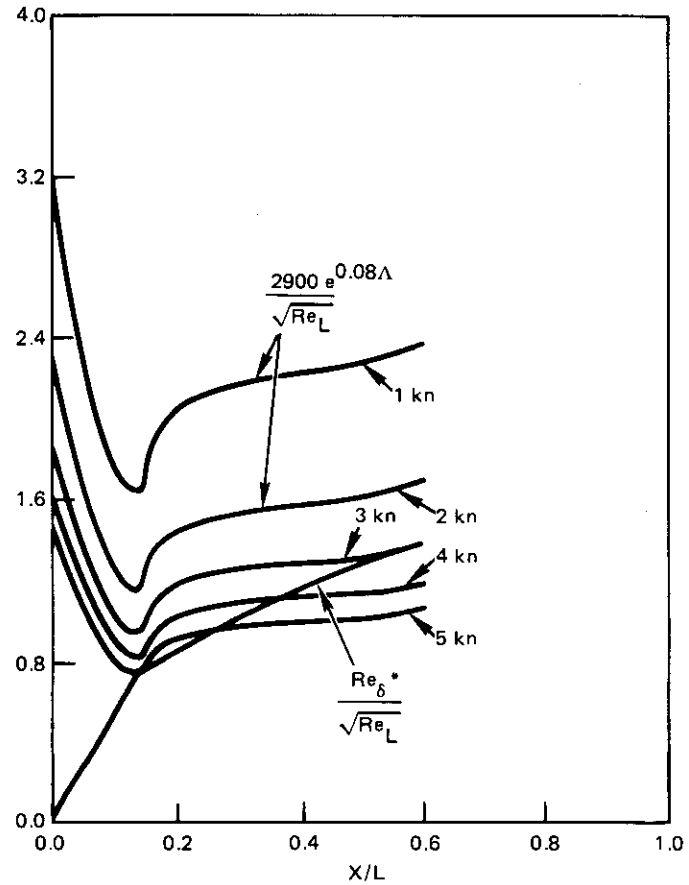

Figure 7. $Re_\delta^*/\sqrt{Re_L}$ and the quantity $2900 \exp(0.08\Lambda)/\sqrt{Re_L}$ for vehicle speeds of 1 to 5 knots.

Speed, Knots	Transition Location X/L	Transition Reynolds No. Re_{xtr}
1	0.5	831000
2	0.5	1.66×10^6
3	0.5	2.49×10^6
4	0.35	2.33×10^6
5	0.25	2.08×10^6

Table 2. Transition location.

Turbulent boundary layer skin friction to the point of cylinder-tail body intersection can be quickly approximated by using the Prandtl-Schlichting skin friction formula

$$C_f = \frac{0.455}{(\log_{10} Re_x)^{2.58}} - \frac{A}{Re_x} \quad . \tag{51}$$

This formula is strictly accurate only for flat plates. However, since for this case, turbulent flow is only being considered on the cylindrical section of the vehicle and the boundary layer thickness is much less than the vehicle diameter, Equation 51 seems to be a reasonable approximation. In Equation 51 the variable A is an allowance for the initial length of laminar flow which varies with transition Reynolds number. Table 3 is reproduced from Schlichting[10] and shows the variation of A with transition Reynolds number.

Re_{xt}	A
3×10^5	1050
5×10^5	1700
1×10^6	3300
3×10^6	8700

Table 3. Laminar flow length allowance.

Calculation of the skin friction coefficient for speeds from 1 to 5 knots is shown in Table 4.

Speed, knots	Re_{xt}	A	Re_x	C_f	C_{D_o}
1	831000	2800	1.32×10^6	2.13×10^{-3}	0.0662
2	1.66×10^6	5300	2.64×10^6	1.74×10^{-3}	0.0541
3	2.49×10^6	7500	3.96×10^6	1.61×10^{-3}	0.0500
4	2.33×10^6	7000	5.28×10^6	2.01×10^{-3}	0.0625
5	2.08×10^6	6400	6.59×10^6	2.24×10^{-3}	0.0696

Table 4. Skin friction coefficient.

10. Schlichting, H., Boundary Layer Theory, McGraw-Hill, 7th Ed., 1979, pg. 641, (equation 21.16a).

The quantity C_f is the skin friction coefficient based on wetted area (A_w). A more convenient drag coefficient (C_{D_o}) is based on the frontal area of the vehicle and can be calculated from the following,

$$C_{D_o} = \frac{C_f A_w}{(\pi/4)D^2} \quad , \tag{52}$$

where again D is simply the vehicle maximum diameter.

From Hoerner[6] the drag coefficient (based on frontal area) of a pointed tail with a length/diameter ratio of 2 at a length Reynolds of 10×10^6 is about 0.038. Approximately one-half of this drag is skin friction and the other half is pressure drag. Using Equation 51 to estimate the percentage increase in skin friction on the tail due to the smaller Reynolds number involved results in afterbody drag coefficient as listed in Table 5.

Speed, Knots	C_{D_o}
1	0.045
2	0.0435
3	0.0420
4	0.0405
5	0.039

Table 5. Afterbody drag coefficient.

The frictional drag of the horizontal and vertical fins was estimated using Equation 51 and assuming totally turbulent flow (thus A = 0). A first design of the fins had rather wide blunt trailing edge ($C_D \cong 0.5$, Hoerner) and preliminary calculations showed that the base (pressure) drag of this design was about four times greater than skin friction alone. The final design has a fairing at the trailing edge, thus eliminating most of the base drag. Using an effective fin length of about 3.2 ft (.97 m), a vertical fin wetted area of

4.05 ft^2 (0.377 m^2) and a horizontal fin wetted area of 4.06 ft^2 (0.377 m^2) results in the fin drag coefficients in Table 6.

Speed, Knots	Re (3.2 ft)	C_f, equation 51	C_{D_o}, vertical	C_{D_o}, horizontal
1	$.34 \times 10^6$	5.51×10^{-3}	.0125	.0125
2	$.68 \times 10^6$	4.81×10^{-3}	.0109	.0109
3	1.02×10^6	4.45×10^{-3}	.0101	.0101
4	1.36×10^6	4.25×10^{-3}	.0096	.0096
5	1.70×10^6	4.06×10^{-3}	.0092	.0092

Table 6. Fin drag coefficients.

The drag coefficients of Table 6 include an allowance for fin-hull interference drag effects of 10 percent (Hoerner, pp 8-12) of the skin friction.

The drag coefficient for a deep hole in a flat surface based on opening area is about 0.008 (Hoerner, pp 5-10). The drag coefficient for the vertical thruster openings (about 8 in. (0.2 m) top and bottom) is then approximately

$$C_{D_o}\Big)_{\substack{\text{thruster}\\ \text{opening}}} = \frac{2(\pi/4)(8)^2}{(\pi/4)(19)^2}\, 0.008 = 0.0028$$

based on the frontal area of the vehicle.

Assuming the boundary layer flow near the propeller nozzle will be turbulent, Equation 51 can also be used to calculate the skin friction on the nozzles. Since to produce thrust the induced velocity near the propellers must be greater than freestream velocity, an induced velocity of 1.2 U_∞ was somewhat arbitrarily assumed. The wetted surface area of each propeller nozzle is about 0.96 ft^2 (0.086 m^2), then the drag coefficient of the nozzles is

$$C_{D_o}\Big)_{nozzles} = \frac{(1.2)^2\ (0.96)\ (2\ \text{nozzles})\ C_f}{(\pi/4)\ (1.583)^2}$$

where C_f is calculated from Equation 51 and Re_L in Equation 51 is based on nozzle length. Table 7 shows the calculated nozzle drag coefficient as a function of speed.

Speed, knots	$Re_L\Big)_{nozzle}$	$C_f\Big)_{nozzle}$	C_{D_o}
1	53600	0.0083	0.0116
2	107200	0.007	0.0099
3	160800	0.00645	0.0091
4	214400	0.00606	0.0085
5	268000	0.00579	0.0081

Table 7. Nozzle drag coefficient.

As a safety feature, this vehicle is designed with a small amount of positive buoyancy so that in any event the vehicle will eventually rise to the surface. At slow speeds constant depth can be maintained only by use of the vertical thruster; at higher speeds the body can be placed at a small angle of attack to produce the required downforce. From Hoerner (pp 7-17) the induced drag for a slender lifting body (i.e., very low aspect ratio) is

$$C_{Di} = 0.5\ C_L\ \tan\alpha \tag{53}$$

where α is the angle of attack and C_L is the lift coefficient of the body based on planform area. From Equation 29 and the definition of lift coefficient, then for small α

$$C_L = \frac{|Z'_\alpha|\ \alpha L^2}{0.95\ LD} = \frac{|Z'_\alpha|\ \alpha L}{0.95\ D} \tag{54}$$

where the term 0.95 LD represents the approximate planform area of the vehicle. The required angle of attack is approximately

$$\alpha = \frac{F_B}{|Z_\alpha|} = \frac{F_B}{(\rho/2)\ U_\infty^2\ L^2\ |Z'_\alpha|} \tag{55}$$

where F_B is the net buoyancy force. For small angles $\alpha \approx \tan \alpha$ and rearranging Equations 53, 54 and 55 results in

$$C_{D_o}\Big)_{\substack{\text{hull}\\ \text{induced}}} = \frac{0.95LDC_{D_i}}{(\pi/4)D^2} = \frac{0.5F_B^2}{(\rho/2)^2 U_\infty^4 L^2 |Z'_\alpha| (\pi/4)D^2} \tag{56}$$

from the program COEFF, Section 3, the value of $|Z'_\alpha|$ is 0.01872. Table 8 shows the calculated values of α (Equation 55) and C_{D_o} for hull-induced drag (Equation 56) for speeds from 3 to 5 knots for an assumed buoyancy force of 10 lbs. Below about 2.5 knots the required angle of attack becomes excessively large, indicating that the vertical thruster would have to be used at these low speeds to maintain depth.

Speed, knots	α, rad.	C_{D_o}
3	.0869	.0087
4	.0489	.0027
5	.0313	.0011

Table 8. Hull induced drag coefficient.

Table 9 shows the individual contributions to the total drag coefficient of each of the components considered in this study. Additionally, an allowance of 15 percent was added to the total drag coefficient to account for the drag effects of gaps, protuberances, control and/or trim planes (design not finalized at time of writing) etc., which will all contribute to the total drag of the vehicle. From Table 9 it can be seen that the drag coefficient

is a minimum at about 3 knots. This effect is caused by the laminar-turbulent transition location moving forward on the cylinder section at higher speeds and thus exposing more of the wetted surface of that section to higher drag turbulent flow.

Component	C_{D_o} (based on frontal area)				
Speed, knots	1.0	2.0	3.0	4.0	5.0
Nose and Cylinder	.0662	.0541	.0500	.0625	.0696
Afterbody	.045	.0435	.0420	.0405	.039
Vertical Fin	.0125	.0109	.0101	.0096	.0092
Horizontal Fin	.0125	.0109	.0101	.0096	.0092
Vertical Thruster Opening	.0028	.0028	.0028	.0028	.0028
Propeller Nozzles	.0116	.0099	.0091	.0085	.0081
Hull Induced Drag	.0087	.0087	.0087	.0027	.0011
Misc. (15%) (elevators, joints gaps, etc.)	.024	.021	.020	.0205	.021
Total	.183	.162	.153	.157	.160

Table 9. Drag contribution of individual components.

SECTION 5

PROPULSION

The performance characteristics of propellers can be described by the performance parameters

$$K_T = \text{thrust coefficient} = \frac{T}{\rho n^2 d^4} \tag{57}$$

and

$$K_Q = \text{torque coefficient} = \frac{Q}{\rho n^2 d^5} \tag{58}$$

which are both a function of

$$J = \text{advance ratio} = \frac{U_a}{nd} \quad . \tag{59}$$

The variable T is propeller thrust, ρ is fluid density, n is propeller shaft speed, d is propeller diameter, Q is torque and U_a is speed of advance of the propeller.

The propellers to be used on the submersible have a diameter d of 7.5 in. (190.5 mm) and an approximate pitch p of 10.6 in. (269 mm) for a pitch ratio of p/d of 1.41. The approximate blade area ratio (BAR) of these propellers is 0.58. Figure 8 shows the approximate curve of K_T versus J for these propellers. This curve was interpolated from Gawn[11] from his performance curves of three bladed propellers with BAR of 0.50 and 0.65 and pitch ratios ranging from 0.4 to 2.0. Figure 9 is likewise the interpolated curve of K_Q versus J. These propellers are installed in flow accelerating (Kort) nozzles which have the effect of increasing K_T (and efficiency) at small values of J and decreasing K_T at high values of J (the latter effect is due to nozzle drag,

---

11. Gawn, R. W. L., Effect of Pitch and Blade Width on Propeller Performance, Paper #6, Institution of Naval Architects, September 29, 1952.

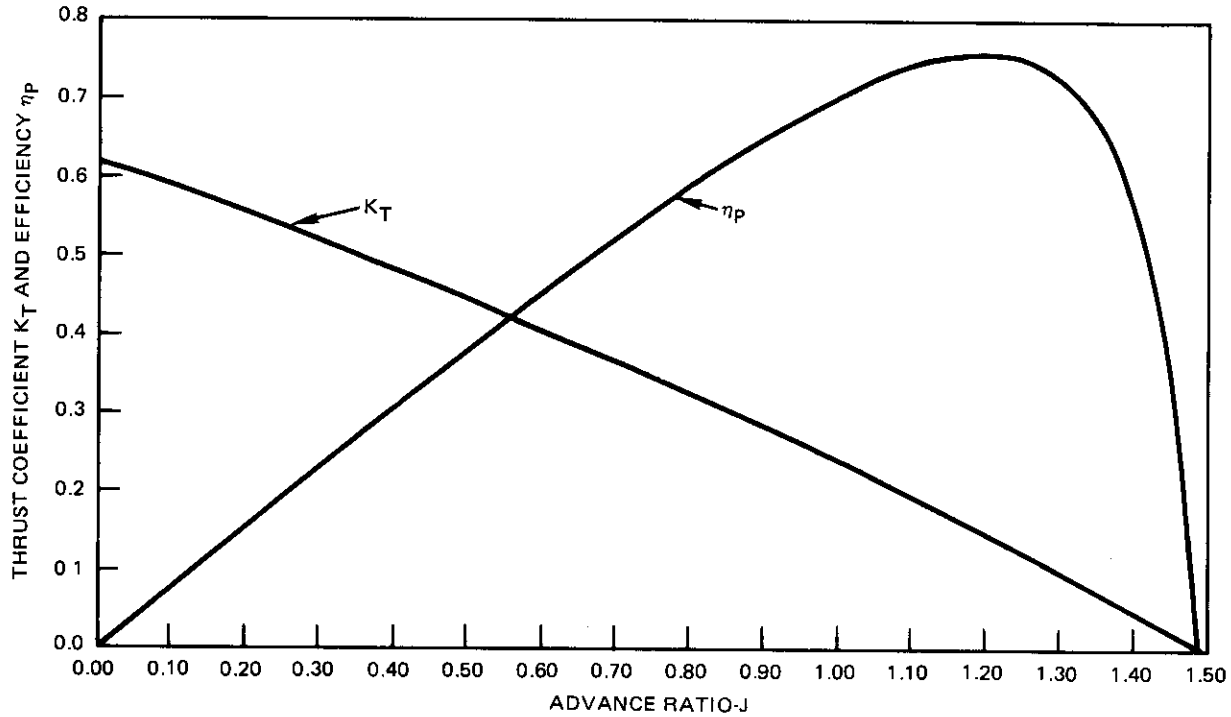

Figure 8. Thrust coefficient K_T and propeller efficiency η_P versus advance ratio J, 3 blade BAR = .58 p/d = 1.41.

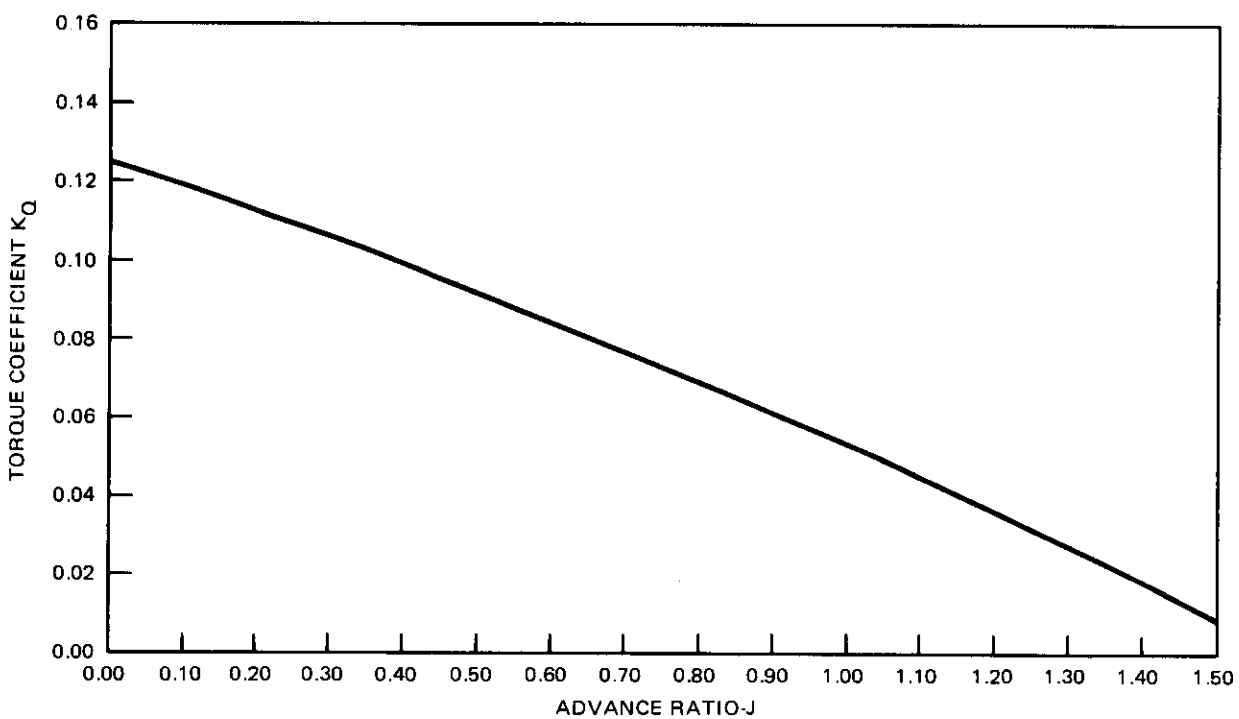

Figure 9. Torque coefficient K_Q versus advance ratio J, 3 blade BAR = .58, p/d = 1.41.

which was taken into account in the calculation of drag coefficient). Since no engineering data exist on the performance of this particular nozzle design, the effect of the nozzle was ignored in this analysis. The error involved in neglecting the nozzle is estimated to be no greater than five percent on the variables K_T and K_Q (for medium values of J). This could lead to an error in calculated maximum speed of about three percent.

The actual thrust produced by propellers is usually required to be somewhat greater than the vehicle drag due to the low pressure exerted on the vehicle hull by the inflow into propellers. Likewise the flow velocity experienced by the propellers is usually less than vehicle speed due to the influence of the wake of the vehicle. These effects are typically accounted for by the thrust deduction t and the wake fraction w, respectively. These factors can usually only be determined by tow tank model test. By definition (for T parallel to drag)

$$\text{Drag} = 0.5\rho U_\infty^2 \, C_{D_o} \, A_o = T(1-t) \tag{60}$$

and

$$U_a = U_\infty \, (1-w) \quad . \tag{61}$$

For a vehicle with constant drag coefficient and thrust divided equally between two propellers canted at angle β then

$$K_{TP} = \frac{0.25 \, J^2 \, C_{D_o} \, A_o}{(1-t) \, d^2 \, \cos\beta \, (1-w)^2} \tag{62}$$

where K_{TP} is the thrust coefficient per propeller.

Linked with propeller performance is the characteristics of the drive motor. The drive motors are permanent magnet (PM) type rated at 1/4 HP at 1000 RPM, 24 VDC 11.1 amps (Q = 252 oz-in) and a no-load speed of 1655 RPM

(0.7 amp). Reference 12 indicates that PM type DC motors have very linear torque-speed and current draw characteristics, such that the motor performance can be expressed as

$$RPM = 1655 - 2.637\ Q\ (oz\text{-}in)$$

or (63)

$$n(rps) = 27.58 - 8.438\ Q\ (lb\text{-}ft)$$

and

$$current = I = 0.7 + 0.0413\ Q\ (oz\text{-}in) \tag{64}$$

or

$$I = 0.7 + 7.929\ Q\ (lb\text{-}ft) \quad .$$

The power output and motor efficiency can be derived from Equation 63 and Equation 64, then

$$horsepower = HP - 0.315\ Q - 0.0964\ Q^2 \tag{65}$$

and

$$motor\ efficiency = \eta_m = \frac{Q(13.984 - 4.278\ Q)}{1 + 11.32\ Q} \quad . \tag{66}$$

Curves of these equations are plotted in Figure 10.

---

12. DC Motors, Speed Controls, Servo Systems, Electro-Craft Corp., 1600 2nd St., Hopkins, MN 55343, August 1980.

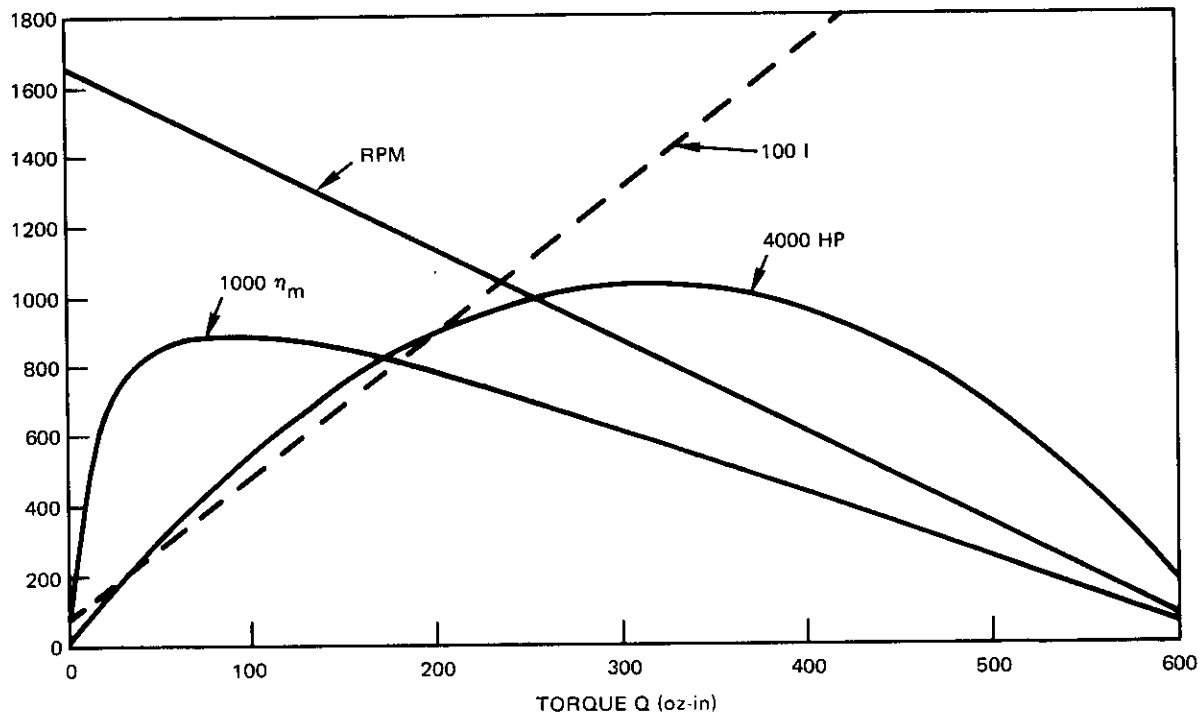

Figure 10. Motor RPM, power output HP, current Draw I and efficiency η_m versus torque Q motor type Minnesota Electric Technology Inc., C32-BB-2, 24 VDC.

For an expected maximum speed of about 5 knots C_{D_o} = 0.16 (from Table 9) and using

$A_o = \Pi D^2/4 = 1.969\ ft^2\ (0.1829\ m^2)$

$d = 0.625\ ft\ (1.1905\ m)$

$\beta = 15°$

$t = w = 0.15$ (best guess)

then for the present vehicle configuration (from Equation 62)

$$K_{TP} = 0.340J^2$$

which from Figure 8 has a solution at J = 0.902, K_{TP} = .278. Then from Figure 8, K_Q = 0.0605 and from the definition of K_Q (Equation 58) and the speed-torque characteristics of the motor (Equation 63) then

$$0.0605 = \frac{Q}{1.9933\ \eta^2\ 0.625^5} = \frac{27.58 - \eta}{8.438\ (1.9933)\ \eta^2\ 0.625^5}$$

which has a positive solution at η = 12.48 rev/sec (749 RPM). From Equation 63, Q = 1.7895 lb ft (2.426 N-m). From Equation 59

$$U_\infty = \frac{Jnd}{1-w} = \frac{0.902\ (12.48)\ 0.625}{1 - .15}$$

$$= 8.277 \text{ ft/sec}$$

$$= 2.523 \text{ m/sec}$$

$$= 4.9 \text{ knots.}$$

The thrust from each propeller can be found from Equation 57

$$T_p = K_{TP}\ n^2 d^4 = .278\ (1.9933)\ (12.48)^2\ (.625)^4$$

$$= 13.17 \text{ lb } (58.58 \text{ N}).$$

Since the values of t and w equal to 0.15 are only a guess, the above calculations were repeated for t = w = 0.05* to see how big an affect this has on vehicle performance. For this case

K_{TP} = 0.238

J = .99

K_Q = 0.053

η = 13.07 rev/sec (784 RPM)

U_∞ = 8.513 ft/sec = 2.595 m/sec = 5.04 knots.

---

*The thrust deduction and wake fraction of marine vehicles usually have values that are almost equal; even though they both can be as large as 0.40 for very full bodied ships.

The above values are only slightly different than for $t = w = 0.15$, which are probably more realistic values for thrust deduction and wake fraction.

From Equation 57 to Equation 59, it follows that

$$\text{propeller efficiency} = \eta = \frac{K_{Tp} J}{2 \Pi K_Q} . \tag{67}$$

For the case where $t = w = 0.15$

$$\eta_p = 0.707 .$$

From Equation 64

$$I = 14.88 \text{ A}$$

and from Equation 65 and Equation 66

$$HP = 0.255$$

$$\eta_m = 0.533.$$

SECTION 6

CONCLUSIONS

The addition of a hydrodynamic fairing to the NOSC free-swimming submersible will significantly increase the top speed of the vehicle to a maximum of approximately 5 knots. Additionally, since in general power required increases at a rate proportional to vehicle speed cubed (at constant drag coefficient), the power required to propel the faired vehicle at the present maximum speed of 1.8 knots will be about 20 times less than on the present vehicle configuration. Therefore, the design of the nose should provide a significant portion of low drag laminar flow over the forward part of the body. This effect will be especially noticeable in the 3 to 4 knot speed region. The size of the vehicle fins is sufficiently large to ensure dynamic stability over the intended speed range. The calculated drag coefficient (0.16 at 5 knots, based on frontal area) is about as low as could be expected given the rather harsh hydrodynamic constraint that the vehicle midsection must be cylindrical. Although a 15 percent "fudge factor" was added to account for drag of small items (i.e., gaps, protuberances, etc., ad infinitum) that could not be accounted for in this report, care needs to be taken in the detail design and final fabrication such that the predicted low drag performance is achieved. Particular attention should be paid to the following details:

- Rivet and/or screw heads should be flush with the vehicle surface. This is particularly important on the forward portion of the vehicle.

- Gaps, joints and steps should be kept to a minimum. Where necessary, joints parallel to the flow are better than joints perpendicular to the flow. Likewise "backward" facing steps are better than "forward" facing steps.

- An effort should be made to minimize turbulence causing leaks through unsealed gaps or holes in the fairing. (Leaks can be caused by the differences between the hydrodynamic pressure on different points on the body (0.5 psi maximum at 5 knots).)

- Avoid sharp corners and blunt trailing edges on any control surfaces or appendages. More generally, avoid any shapes from which the flow will separate causing large increments of pressure drag.

The existing motor and propeller combination seem to be fairly well matched to the anticipated vehicle drag and speed. The propellers will be operating near their peak efficiency ($J = 0.902$, $\eta_p = .707$) and the motors near their peak power (.255 HP at 749 RPM).

SECTION 7

REFERENCES

1. Heckman, Paul J., Jr., Free-Swimming Submersible Testbed (EAVE WEST) Naval Ocean Systems Center TR 622, September 1980.

2. Parsons, J. S., Goodson, R. E. and Goldschmied, F. R., Shaping of Axisymmetric Bodies for Minimum Drag in Incompressible Flow, J. of Hydronautics, Vol. 8, No. 3, July 1974, pp. 100-107.

3. Cebeci, T. and Bradshaw, P., Momentum Transfer in Boundary Layers, McGraw-Hill, 1977, pg. 108.

4. Friedman, D. M., Improved Solution for Potential Flow about Arbitrary Axisymmetric Bodies by the use of a Higher Order Surface Source Method, Part II, User's Manual for Computer Program, NASA CR 134695, July 1974.

5. White, F. M., Viscous Fluid Flow, McGraw-Hill, 1974, pg. 432 (Equation 5-39), pg. 316.

6. Hoerner, Sighard F., Fluid-Dynamic Drag, Published by the author, 1965, pg. 20-2, pg. 3-12, pg. 8-12, pg. 7-17.

7. Arentzen, E. S. and Mandel, P., Naval Architectural Aspects of Submarine Design, Trans SNAME, 1960.

8. Comstock, J. P., ed., Principles of Naval Architecture, SNAME, 1967, Chapter VIII.

9. Bottaccini, M. R., The Stability Coefficients of Standard Torpedoes, NAVORD Report 3346, 1954.

10. Schlichting, H., Boundary Layer Theory, McGraw-Hill, 7th Ed., 1979, pg. 641 (Equation 21.16a).

11. Gawn, R. W. L., Effect of Pitch and Blade Width on Propeller Performance, Paper #6, Institution of Naval Architects, September 29, 1952.

12. DC Motors, Speed Controls, Servo Systems, Electro-Craft Corp., 1600 2nd St., Hopkins, MN 55343, August 1980.

APPENDIX

Program Listings
and Sample Run

```
@PRT POTEN.COORD/FTN
FURPUR 28R2 S74R1A 10/13/82 08:45:39
SWEM*POTEN(1).COORD/FTN(15)
      DIMENSION X(500),R(500),ANG(500)
      CHARACTER HEADER(60),CASE(6)
C DATA FOR CONTROL CARD 2 OF DOUGLAS PROGRAM
      DATA NB,NNU,IAXI,ICROSS,IOFF,IONLY,IELPSE/1,0,1,0,0,0,0/
      DATA IPRTRB,IPOTNL,IPTANV,IVORT,IOMITA,IOMITC/6*0/
      DATA ISURFV,IPRSCV,IALLV,IEXCRS,IGENBC,IRNGW/6*0/
      DATA IPNCH,IUNIT,IVIJ,ICOEF,IPRINT,IRAKF/1,5,4*0/
C DATA FOR CONTROL CARD 3
      DATA CHORD,XMACH/1.0,0.0/
C DATA FOR CONTROL CARD 4
      DATA IGEOMF,ISIGF,ICURVN,NONEWF,IFORMT/0,0,0,0,2/
      DATA XMULT,YMULT,THETA,ADDX,ADDY/1.0,1.0,0.0,0.0,0.0/
C.DATA FOR CARD 5
      DATA IBDN,ISUBKS,NLF,A,B/1,0,0,0.0,0.0/
      WRITE(6,100)
  100 FORMAT(1X,'COORDINATE GENERATION PROGRAM FOR DOUGLAS')
      WRITE(6,101)
  101 FORMAT(1X,'AXISYMETRIC POTENTIAL FLOW PROGRAM.  FUNCTION RVSX')
      WRITE(6,102)
  102 FORMAT(1X,'(I.E. RADIUS VS. X) SHOULD BE COMPILED AND LINKED')
      WRITE(6,103)
  103 FORMAT(1X,'BEFORE EXECUTION')
      DSMAX=0.01
      DANGLE=5.0
      ANOSE=90.0
      WRITE(6,125)CHORD
  125 FORMAT(1X,'INPUT REF. CHORD <',F8.4,'>')
      READ(5,210)ANS
      IF(ANS.NE.0.)CHORD=ANS
      WRITE(6,126)XMACH
  126 FORMAT(1X,'INPUT MACH NO. <',F8.4,'>')
      READ(5,210)XMACH
      WRITE(6,150)ANOSE
  150 FORMAT(1X,'INPUT NOSE ANGLE (90.=BLUNT) <',F7.3,'>')
      READ(5,210)ANS
      IF(ANS.NE.0.)ANOSE=ANS
      WRITE(6,200)DSMAX
  200 FORMAT(1X,'INPUT MAX. SURFACE STEP <',F8.4,'>')
      READ(5,210)ANS
  210 FORMAT(F10.4)
      IF(ANS.NE.0.)DSMAX=ANS
      WRITE(6,220)DANGLE
  220 FORMAT(1X,'INPUT MAX. SLOPE CHANGE (DEGREES)<',F8.4,'>')
      READ(5,210)ANS
      IF(ANS.NE.0.)DANGLE=ANS
  250 RANGLE=DANGLE/57.2977951
      NN=1
      X(1)=0.
      R(1)=0.
      ANG(1)=ANOSE/57.29577951
      DX=DSMAX
      I=NN
  300 IF(X(I)+DX.GT.CHORD)GO TO 500
      IF(INDEX.EQ.500)GO TO 400
```

```
      NN=NN+1
      I=NN
      DX=DSMAX
  350 X(I)=X(I-1)+DX
      R(I)=RVSX(X(I))
      DR=R(I)-R(I-1)
      DS=SQRT(DX*DX+DR*DR)
      ANG(I)=ATAN(DR/DX)
      ANGCHK=ABS(ANG(I)-ANG(I-1))
      IF(ANGCHK.LE.RANGLE.AND.DS.LE.DSMAX)GO TO 300
      DX=0.9*DX
      IF(DX.LT.0.0001*DSMAX)GO TO 450
      GO TO 350
  400 DANGLE=1.1*DANGLE
      DSMAX=1.1*DSMAX
      WRITE(6,410)DSMAX,DANGLE
  410 FORMAT(1X,'MORE THAN 500 POINTS!!, CHANGING MAX. SURFACE STEP'./
     1,1X,'TO',F8.4,' AND MAX. SLOPE TO',F8.4)
      GO TO 250
  450 WRITE(6,460)I
  460 FORMAT(1X,'DX TOO SMALL FOR POINT',I5,' PROCEEDING ANYWAY!')
      GO TO 300
  500 WRITE(6,510)NN
  510 FORMAT(//,1X,'NO. OF POINTS FOR THIS RUN=',I4,//)
      WRITE(6,520)
  520 FORMAT(5X,'X/C',16X,'R/C',/)
      DO 600 I=1,NN
  600 WRITE(6,550)X(I),R(I)
  550 FORMAT(1X,F10.5,10X,F10.5)
      WRITE(6,700)
  700 FORMAT(1X,'BEGINNING OUTPUT TO UNIT 17.  INPUT HEADER?')
      READ(5,720)HEADER
  720 FORMAT(60A1)
      WRITE(6,730)
  730 FORMAT(1X,'INPUT CASE NO.')
      READ(5,740)CASE
  740 FORMAT(6A1)
      WRITE(17,750)HEADER,CASE
  750 FORMAT(60A1,6A1)
      WRITE(17,760)NB,NNU,IAXI,ICROSS,IOFF,IONLY,IELPSE,IPRTB,IPOTNL,
     1IPTANV,IVORT,IOMITA,IOMITC,ISURV,IPRSCV,IALLV,IEXCRS,
     2IGENBC,IRNGW,IPNCH,IUNIT,IVIS,ICOEF,IPRINT,IRAKF
  760 FORMAT(7I1,3X,2I1,I2,9I1,4X,I1,I2,4I1)
      WRITE(17,770)CHORD,XMACH
  770 FORMAT(2F10.6)
      WRITE(17,780)IGEOMF,ISIGF,ICURVN,NONEWF,IFORMT,NN,XMULT,YMULT,
     1THETA,ADDX,ADDY
  780 FORMAT(5I1,I5,5F10.5)
      WRITE(17,790)IBDN,ISUBKS,NLF,A,B
  790 FORMAT(3I10,2F10.5)
      DO 800 I=1,NN
      WRITE(17,810)X(I),R(I)
  810 FORMAT(F10.6,10X,F10.6)
  800 CONTINUE
      ENDFILE 17
      END
```

```
@PRT POTEN.LAMINR/FOR
SWEM*POTEN(1).LAMINR/FOR(17)
      DIMENSION XOL(401),RTORRL(401),H(401),DTORRL(401),CLAMDA(401)
      DIMENSION ROL(401),SOL(401),VRATIO(401)
      DIMENSION CARY(2),ZTRANS(500)
      COMMON NXT,KASE,BIGL,CNU,S(500),X(500),R(500),UE(500)
      NPOINT=401
      NXT=500
      KASE=2
      KDIS=0
      UREF=1.0
      RL=1.0
      CNU=1.0
      BIGL=1.0
      Q=FLOAT(NPOINT-1)
      WRITE(6,45)
   45 FORMAT(///,7X,'I',10X,'X/L',9X,'R/L',6X,'VRATIO')
      XSTEP=BIGL/Q
      ROL(1)=0.
      H(1)=2.429
      CLAMDA(1)=0.052
      RTORRL(1)=0.
      DTORRL(1)=0.
       SOL(1)=0.
      DO 100 I=1,NPOINT
      Q=NPOINT-1
      XOL(I)=BIGL*FLOAT(I-1)/Q
      VRATIO(I)=UEUINF(XOL(I))
      ROL(I)=RVSX(XOL(I))
  100 WRITE(6,55)I,XOL(I),ROL(I),VRATIO(I)
   55 FORMAT(5X,I5,3F12.4)
      IXPOS=2
  150 NXT=500
      IF(IXPOS.LT.20)NXT=100
      UE(1)=0.
      R(1)=0.
      X(1)=0.
      Q=NXT-1
      XSTEP=XOL(IXPOS)/Q
      DO 250 I=2,NXT
      X(I)=FLOAT(I-1)*XSTEP*BIGL
      R(I)=RVSX(X(I))*BIGL
      UE(I)=UEUINF(X(I)/BIGL)*UREF
  250 CONTINUE
      CALL THWTES(KDIS,UREF,DELS,THETA,H(IXPOS),CF,RTHETA,RS,
     1CLAMDA(IXPOS))
      RTORRL(IXPOS)=RTHETA/SQRT(RL)
      DTORRL(IXPOS)=H(IXPOS)*RTORRL(IXPOS)
      SOL(IXPOS)=S(NXT)/BIGL
      NSEP=IXPOS
      IF(IXPOS.EQ.NPOINT-1.OR.CLAMDA(IXPOS).LT.-0.09)GO TO 300
      IXPOS=IXPOS+1
      GO TO 150
  300 NSEP=NSEP-1
      IF(NSEP.GT.240)NSEP=240
      WRITE(6,305)
  305 FORMAT(//,7X,'X/L',4X,'RHTETA',7X,'H',8X,'RDEL',5X,'LAMDA')
```

```
      DO 350 I=1,NSEP
      WRITE(6,310)XOL(I),RTORRL(I),H(I),DTORRL(I),CLAMDA(I)
  310 FORMAT(4F10.3,F10.4)
  350 CONTINUE
      P1X=1.5
      P1Y=6.0
      P2X=P1X
      P2Y=1.0
      XMAX=1.0
      YMAX=2.0
      BLOWX=1.0
      XAXIS=6.0
      YAXIS=4.0
      IPLOT=IPLOT+1
      CALL BGNPL(IPLOT)
      CALL PHYSOR(P1X,P1Y)
      CALL TITLE('VELOCITY RATIO$',100,'X/L',3,'UE/UINF$',100,XAXIS
     1,YAXIS)
      CALL GRAF(0.0,XMAX/5.0,XMAX,0.0,YMAX/5.0,YMAX)
      CALL GRID(1,1)
      CALL CURVE(XOL,VRATIO,NPOINT,0)
      SCALEF=(XAXIS/XMAX)*(YMAX/YAXIS)
      CALL BSCALE(1.0,SCALEF)
      CALL CURVE(XOL,ROL,NPOINT,0)
      CALL BSCALE(1.0,1.0)
      CALL ENDGR(IPLOT)
      IPLOT=IPLOT+1
      CALL PHYSOR(P2X,P2Y)
      CALL RETITL
      IPOINT=INT(FLOAT(NPOINT)/BLOWX)
      XBMAX=XMAX/BLOWX
      CALL GRAF(0.0,XBMAX/5.0,XBMAX,0.0,YMAX/5.0,YMAX)
      CALL GRID(1,1)
      CALL CURVE(XOL,VRATIO,IPOINT,0)
      CALL BSCALE(1.0,SCALEF*BLOWX)
      CALL CURVE(XOL,ROL,IPOINT,0)
      CALL BSCALE(1.0,1.0)
      CALL ENDPL(IPLOT)
      IPLOT=IPLOT+1
      CALL BGNPL(IPLOT)
      CALL PHYSOR(P1X,P1Y)
      CALL TITLE('BOUNDARY LAYER PARAMETERS$',100,'X/L',3,' ',1
     1,XAXIS,YAXIS)
      CALL GRAF(0.0,XBMAX/5.0,XBMAX,0.0,0.8,4.0)
      CALL GRID(1,1)
      CALL CURVE(XOL,RTORRL,NSEP,0)
      CALL HEIGHT(0.07)
      XMESS=XOL(NSEP)+.015
      CALL RLMESS('RE THETA/SQRT(RE L)$',100,XMESS,RTORRL(NSEP))
      CALL CURVE(XOL,DTORRL,NSEP,0)
      CALL RLMESS('RE DELTA/SQRT(RE L)$',100,XMESS,DTORRL(NSEP))
      CALL CURVE(XOL,H,NSEP,0)
      CALL RLMESS('H',1,XMESS,H(NSEP))
      CALL ENDGR(IPLOT)
      IPLOT=IPLOT+1
      CALL PHYSOR(P2X,P2Y)
      CALL HEIGHT(0.14)
```

```
      CALL RETITL
      CALL GRAF(0.0,XBMAX/5.0,XBMAX,-0.1,0.1,0.3)
      CALL GRID(1,1)
      CALL CURVE(XOL,CLAMDA,NSEP,0)
      CALL HEIGHT(0.07)
      CALL RLMESS('LAMDA$',100,XMESS,CLAMDA(NSEP))
      CALL ENDPL(IPLOT)
      IPLOT=IPLOT+1
      CNU=1.575E-05
      BIGL=15.5
      CALL BGNPL(IPLOT)
      CALL TITLE('TRANSITION CURVES$',100,'X/L',3,' ',1,XAXIS,
     12.0*YAXIS)
      CALL GRAF(0.0,XBMAX/5.,XBMAX,0.0,0.8,4.0)
      CALL GRID(1,1)
      CALL CURVE(XOL,DTORRL,NSEP,0)
      CALL HEIGHT(0.07)
      CALL RLMESS('RE DELTA/SQRT(REL)$',100,XMESS,DTORRL(NSEP))
      DO 1000 KNOTS=1,5
      VEL=1.6889*FLOAT(KNOTS)
      RL=BIGL*VEL/CNU
      DO 900 I=1,NSEP
      ZTRANS(I)=2900.*EXP(0.08*BLAMDA(CLAMDA(I)))/SQRT(RL)
  900 CONTINUE
      CALL CURVE(XOL,ZTRANS,NSEP,0)
      ENCODE(12,1200,CARY,IDUM)KNOTS
 1200 FORMAT('ZTRANS',I2,'KT. ')
      CALL RLMESS(CARY,12,XMESS,ZTRANS(NSEP))
 1000 CONTINUE
      CALL DONEPL
      END
```

```
@PRT POTEN.RVSX/PGG
SWEM*POTEN(1).RVSX/PGG(18)
      FUNCTION RVSX(X)
C RADIUS FUNCTION USING PARSONS,GOODSON AND GOLDSCHMIED EQUATION
C FOR NOSE SHAPE AND A CIRCULAR ARC TAIL SECTION
C THE FOLLOWING ARE FUNCTIONS 4C,4D,4E OF PGG.
      F1(Z)=(-2.0*Z*(Z-1.0)**3)
      F2(Z)=(-(Z*Z)*(Z-1.0)*(Z-1.0))
      G(Z)=Z*Z*(3.0*Z*Z-8.0*Z+6.0)
C CHORD=LENGTH OF BODY
      CHORD=1.0
C ALEN=FINESS RATIO    CHORD/DIAMETER
      ALEN=9.7895
      RMAX=0.5*CHORD/ALEN
C RNOSE=NOSE CURVATURE (SAME UNITS AS CHORD)
      RNOSE=(4./7.)*RMAX
C AK1=CURVATURE AT INTERSECTION OF NOSE AND CYLINDER
C I.E.    DY**2/DX**2 AT INTERSECTION OF NOSE AND CYLINDER
      AK1=0.
C TAILSZ=LENGTH OF TAILCONE/MAX. RADIUS
      TAILSZ=4.
C ARCCEN=Y COORD. OF CENTER OF TAILCONE ARC (I.E. DISTANCE
C BELOW CENTERLINE OF ARC CENTER
      ARCCEN=0.5*RMAX*(TAILSZ*TAILSZ-1.0)
```

```
C XMAXDS=DISTANCE FROM NOSE TO INTERSECTION OF NOSE AND CYLINDER SECTION
      XMAXDS=3.0*RMAX
C DRNOSE AND DK1 ARE THE APPROPRIATE DIMENSIONLESS CURVATURES
      DRNOSE=4.0*XMAXDS*RNOSE*(ALEN/CHORD)**2
      DK1=(-XMAXDS*XMAXDS/RMAX)*AK1
C XMAXDE IS X ORDINATE OF START OF TAILCONE
      XMAXDE=2.0*ALEN*RMAX-TAILSZ*RMAX
      IF(X.LE.0.)GO TO 100
      IF(X.GT.0..AND.X.LT.XMAXDS)GO TO 200
      IF(X.GE.XMAXDS.AND.X.LT.XMAXDE)GO TO 300
      IF(X.GE.XMAXDE.AND.X.LE.CHORD)GO TO 400
  100 RVSX=0.
      RETURN
  200 XF=X/XMAXDS
      RVSX=CHORD*SQRT(DRNOSE*F1(XF)+DK1*F2(XF)+G(XF))/(2.0*ALEN)
      RETURN
  300 RVSX=RMAX
      RETURN
  400 RVSX=SQRT((ARCCEN+RMAX)**2-(X-XMAXDE)**2)-ARCCEN
      RETURN
      END
```

```
@PRT POTEN.UEUINF/FOR
SWEM*POTEN(1).UEUINF/FOR(8)
      FUNCTION UEUINF(X)
      DIMENSION UE(500),XC(500),YC(500)
C THIS FUNCTION LINEAR INTERPOLATES BETWEEN VELOCITY POINTS
C (AS A FUNCTION OF X).  INPUT POINTS ASSUMED TO BE INPUT ON UNIT 18.
      DATA IREAD/0/
      IF(IREAD.NE.0)GO TO 100
      READ(18,50)NT
   50 FORMAT(I5)
      NLAST=NT+1
      DO 75 I=2,NLAST
   75 READ(18,85)XC(I),YC(I),UE(I)
   85 FORMAT(3F15.8)
      REWIND 18
      IREAD=1
      XC(1)=0.
      YC(1)=0.
      UE(1)=0.
      ILAST=1
  100 IF(X.LT.XC(ILAST))ILAST=1
      IF(X.LT.XC(1).OR.X.GT.XC(NLAST))GO TO 150
  110 IF(XC(ILAST).LE.X.AND.X.LE.XC(ILAST+1))GO TO 200
      ILAST=ILAST+1
      IF(ILAST.LT.NLAST)GO TO 110
  150 ILAST=1
      UEUINF=0.
      RETURN
  200 UEUINF=(UE(ILAST+1)-UE(ILAST))*(X-XC(ILAST))/(XC(ILAST+1)
     1-XC(ILAST))+UE(ILAST)
      RETURN
      END
```

```
@PRT POTEN.THWTES/FOR
SWEM*POTEN(1).THWTES/FOR(0)
      SUBROUTINE THWTES(KDIS,UREF,DELS,THETA,H,CF,RTHETA,RS,CLAMDA)
C     SUBROUTINE TO CALCULATE LAMINAR BOUNDARY LAYER PARAMETERS
C     (THAITES METHOD) CEBECI-SMITH SECTION 5.6.3
C
C     UREF=FREESTREAM VELOCITY, DELS=DISPLACEMENT THICHNESS
C     THETA=MOMENTUM THICKNESS,H=SHAPE FACTOR,CF=LOCAL DRAG COEFF.
C    RTHETA=REYNOLDS NO. (MOMENTUM THICKNESS),CNU=K. VISCOSITY
C     NXT=NO. OF DATA POINTS,KASE=FLOW INDEX,0=2-D,1=2-D STAG
C     2=AXISYMMETRIC FLOW,BIGL=REFERENCE LENGTH
C     DIMENSIONLESS VARIABLES:X=AXIAL OR CHORDWISE DISTANCE,
C     UE=VELOCITY RATIO,R=BODY ORDINATE OR RADIUS,S=SURFACE
C     DISTANCE,RS=REYNOLDS NO.(BASED ON S)
      COMMON NXT,KASE,BIGL,CNU,S(500),X(500),R(500),UE(500)
      IF(KDIS.EQ.1)GO TO 100
      S(1)=0.
      DO 50 I=2,NXT
   50 S(I)=S(I-1)+SQRT((X(I)-X(I-1))**2+(R(I)-R(I-1))**2)
  100 F1=0.
      CF=0.
      URSUM=0.
      RL=UREF*BIGL/CNU
      F2=0.
      DO 500 I=2,NXT
      R2=1.
      IF(KASE.EQ.2)R2=R(I)**2
      F2=UE(I)**5*R2
      URSUM=URSUM+0.5*(F1+F2)*(S(I)-S(I-1))
  500 F1=F2
      DUEDS=(UE(NXT)-UE(NXT-1))/(S(NXT)-S(NXT-1))
      CONST=0.45/(F2*UE(NXT))
      THTATM=CONST+URSUM
      THETA=SQRT(THTATM/RL)*BIGL
      RTHETA=THETA*UE(NXT)/CNU*UREF
      RS=UE(NXT)*S(NXT)/CNU*UREF*BIGL
      CLAMDA=THTATM*DUEDS
      IF(CLAMDA.LT.0.)GO TO 550
      H=2.61-3.75*CLAMDA+5.24*CLAMDA**2
      CL=0.221+1.57*CLAMDA-1.8*CLAMDA**2
      GO TO 600
  550 H=0.0731/(0.14+CLAMDA)+2.088
      CL=0.22+1.402*CLAMDA+0.018*CLAMDA/(CLAMDA+0.107)
  600 DELS=THETA*H
      CF=2.0*CL/(UE(NXT)*THETA/BIGL*RL)
      RETURN
      END
```

```
@ASG,T    1,F/50/TRK/400
READY

@ASG,T    2,F/50/TRK/400
READY

@ASG,T    3,F/50/TRK/400
READY

@ASG,T    4,F/5/TRK/20
READY

@ASG,T    8,F/80/TRK/1100
READY

@ASG,T    9,F/80/TRK/1100
READY

@ASG,T   10,F/80/TRK/1100
READY

@ASG,T   11,F/50/TRK/400
READY

@ASG,T   12,F/5/TRK/20
READY

@ASG,T   13,F/5/TRK/20
READY

@ASG,T   15,F/1/TRK/1
READY

@ASG,T   16,F/1/TRK/1
READY

@USE 1,1
READY

@USE 2,2
READY

@USE 3,3
```

```
READY

@USE 4,4
READY

@USE 8,8
READY

@USE 9,9
READY

@USE 10,10
READY

@USE 11,11
READY

@USE 12,12
READY

@USE 13,13
READY

@USE 15,15
READY

@USE 16,16
READY

@XQT POTEN.COORD/ABS
COORDINATE GENERATION PROGRAM FOR DOUGLAS
AXISYMETRIC POTENTIAL FLOW PROGRAM.  FUNCTION RVSX
(I.E. RADIUS VS. X) SHOULD BE COMPILED AND LINKED
BEFORE EXECUTION
INPUT REF. CHORD <  1.0000>
INPUT MACH NO. <   .0000>
INPUT NOSE ANGLE (90.=BLUNT) < 90.000>
INPUT MAX. SURFACE STEP <   .0100>
INPUT MAX. SLOPE CHANGE (DEGREES)<  5.0000>

NO. OF POINTS FOR THIS RUN=  47

    X/C                R/C

    .00000              .00000
```

```
    .00162              .00965
    .00188              .01041
    .00703              .01968
    .00865              .02168
    .01941              .03107
    .02456              .03421
    .04706              .04307
    .06731              .04728
    .08981              .04970
    .11231              .05074
    .13481              .05105
    .15731              .05108
    .18231              .05108
    .20731              .05108
    .23231              .05108
    .25731              .05108
    .28231              .05108
    .30731              .05108
    .33231              .05108
    .35731              .05108
    .38231              .05108
    .40731              .05108
    .43231              .05108
    .45731              .05108
    .48231              .05108
    .50731              .05108
    .53231              .05108
    .55731              .05108
    .58231              .05108
    .60731              .05108
    .63231              .05108
    .65731              .05108
    .68231              .05108
    .70731              .05108
    .73231              .05108
    .75731              .05108
    .78231              .05108
    .80481              .05098
    .82731              .04992
    .84981              .04769
    .87231              .04426
    .89481              .03961
    .91731              .03370
    .93981              .02646
    .96231              .01783
    .98481              .00772
BEGINNING OUTPUT TO UNIT 17.  INPUT HEADER?
INPUT CASE NO.

@XQT DOUG.HODAPF/ABS
```

```
                    DOUGLAS  AIRCRAFT COMPANY
                      LONG  BEACH  DIVISION

PROGRAM EODF -- PARABOLIC AXISYMMETRIC AND CROSSFLOW

     ***** CASE CONTROL DATA *****

TEST RUN                                                    CASE NO.

BODIES  =  1
NNU     =  0
CHORD   =   1.0000000
MACH NO.=   .00000000
TCNST   =    .0000000
EPSLON =    .0000000
PSF NO. =

        SURFACE OF REVOLUTION
        MATRIX SOLUTION BY TRIANGULARIZATION   (SOLVIT)
        PUNCHED OUTPUT
        INPUT TAPE NO. FOR COORDINATES AND NON-UNIFORM FLOW ONLY =    5
```

DOUGLAS AIRCRAFT COMPANY
LONG BEACH DIVISION

TEST RUN

NN = 47 MX = 1.0000000 MY = 1.0000000
THETA = .0000000 ADDX = .0000000 ADDY = .0000000
XE = .0000000 YE = .0000000

CURVED ELEMENTS(IGEOMF=0) PIECEWISE-PARABOLIC SOURCE DENSITIES(ISIGF=0) INTERNALLY-COMPUTED ELEMENT CURVATURES(ICURVN=0)
NEW VELOCITY FORMULAE ARE USED.

O N - B O D Y C O O R D I N A T E S

	UNTRANSFORMED		*** TRANSFORMED ***							
	X	Y	X	Y	X C.P.	Y C.P.	DELTA S	SUMDS	D ALPHA	CURVATURE
1	.00000	.00000	.00000	.00000						
					.00042	.00489	.00982	.00982	.00000	-32.85389
2	.00162	.00965	.00162	.00965						
					.00175	.01003	.00081	.01063	-10.00610	-30.85161
3	.00189	.01041	.00189	.01041						
					.00412	.01523	.01065	.02128	-9.51128	-27.54357
4	.00703	.01968	.00703	.01968						
					.00782	.02070	.00257	.02385	-9.91280	-23.22262
5	.00865	.02168	.00865	.02168						
					.01372	.02673	.01432	.03817	-9.97205	-18.55179
6	.01941	.03107	.01941	.03107						
					.02195	.03269	.00603	.04420	-9.73967	-13.77279
7	.02456	.03421	.02456	.03421						
					.03556	.03927	.02423	.06843	-9.84897	-9.28072
8	.04706	.04307	.04706	.04307						
					.05712	.04548	.02070	.08913	-9.76530	-5.84842
9	.06731	.04728	.06731	.04728						
					.07853	.04871	.02264	.11176	-5.59522	-3.49200
10	.08981	.04970	.08981	.04970						
					.10105	.05035	.02253	.13429	-3.50000	-1.97620
11	.11231	.05074	.11231	.05074						
					.12356	.05095	.02250	.15679	-1.86219	-.89190
12	.13481	.05105	.13481	.05105						
					.14606	.05107	.02250	.17929	-.71042	-.16992
13	.15731	.05107	.15731	.05107						
					.16981	.05107	.02500	.20429	-.07130	.00000
14	.18231	.05107	.18231	.05107						
					.19481	.05107	.02500	.22929	.00000	.00000
15	.20731	.05107	.20731	.05107						
					.21981	.05107	.02500	.25429	.00000	.00000
16	.23231	.05107	.23231	.05107						
					.24481	.05107	.02500	.27929	.00000	.00000
17	.25731	.05107	.25731	.05107						
					.26981	.05107	.02500	.30429	.00000	.00000
18	.28231	.05107	.28231	.05107						
					.29481	.05107	.02500	.32929	.00000	.00000
19	.30731	.05107	.30731	.05107						
					.31981	.05107	.02500	.35429	.00000	.00000

20	.33231	.05107	.33231	.05107	.34481	.05107	.02500	.37929	.00000	.00000
21	.35731	.05107	.35731	.05107	.36981	.05107	.02500	.40429	.00000	.00000

DOUGLAS AIRCRAFT COMPANY
LONG BEACH DIVISION

TEST RUN

NN = 47 MX = 1.0000000 MY = 1.0000000
THETA = .0000000 ADDX = .0000000 ADDY = .0000000
XE = .0000000 YE = .0000000

CURVED ELEMENTS(IGEOMF=0) PIECEWISE-PARABOLIC SOURCE DENSITIES(ISIGF=0) INTERNALLY-COMPUTED ELEMENT CURVATURES(ICURVN=0)
NEW VELOCITY FORMULAE ARE USED.

O N - B O D Y C O O R D I N A T E S

	UNTRANSFORMED		*** TRANSFORMED ***							
	X	Y	X	Y	X C.P.	Y C.P.	DELTA S	SUMDS	D ALPHA	CURVATURE
22	.38231	.05107	.38231	.05107						
					.39481	.05107	.02500	.42929	.00000	.00000
23	.40731	.05107	.40731	.05107						
					.41981	.05107	.02500	.45429	.00000	.00000
24	.43231	.05107	.43231	.05107						
					.44481	.05107	.02500	.47929	.00000	.00000
25	.45731	.05107	.45731	.05107						
					.46981	.05107	.02500	.50429	.00000	.00000
26	.48231	.05107	.48231	.05107						
					.49481	.05107	.02500	.52929	.00000	.00000
27	.50731	.05107	.50731	.05107						
					.51981	.05107	.02500	.55429	.00000	.00000
28	.53231	.05107	.53231	.05107						
					.54481	.05107	.02500	.57929	.00000	.00000
29	.55731	.05107	.55731	.05107						
					.56981	.05107	.02500	.60429	.00000	.00000
30	.58231	.05107	.58231	.05107						
					.59481	.05107	.02500	.62929	.00000	.00000
31	.60731	.05107	.60731	.05107						
					.61981	.05107	.02500	.65429	.00000	.00000
32	.63231	.05107	.63231	.05107						
					.64481	.05107	.02500	.67929	.00000	.00000
33	.65731	.05107	.65731	.05107						
					.66981	.05107	.02500	.70429	.00000	.00000
34	.68231	.05107	.68231	.05107						
					.69481	.05107	.02500	.72929	.00000	.00000
35	.70731	.05107	.70731	.05107						
					.71981	.05107	.02500	.75429	.00000	.00000
36	.73231	.05107	.73231	.05107						
					.74481	.05107	.02500	.77929	.00000	.00000
37	.75731	.05107	.75731	.05107						
					.76981	.05107	.02500	.80429	.00000	.00000
38	.78231	.05107	.78231	.05107						
					.79356	.05106	.02250	.82679	-.24191	-.58081
39	.80481	.05098	.80481	.05098						
					.81606	.05058	.02253	.84932	-2.44774	-2.09040
40	.82731	.04992	.82731	.04992						
					.83857	.04895	.02261	.87193	-2.97808	-2.30252

41	.84981	.04769	.84981	.04769	.86108	.04612	.02276	.89469	-2.99250	-2.30301
42	.87231	.04426	.87231	.04426	.88359	.04209	.02298	.91767	-3.01895	-2.30393

DOUGLAS AIRCRAFT COMPANY
LONG BEACH DIVISION

TEST RUN

NN = 47 MX = 1.0000000 MY = 1.0000000
THETA = .0000000 ADDX = .0000000 ADDY = .0000000
XE = .0000000 YE = .0000000

CURVED ELEMENTS(IGEOMF=0) PIECEWISE-PARABOLIC SOURCE DENSITIES(ISIGF=0) INTERNALLY-COMPUTED ELEMENT CURVATURES(ICURVN=0)
NEW VELOCITY FORMULAE ARE USED.

O N - B O D Y C O O R D I N A T E S

	UNTRANSFORMED		*** TRANSFORMED ***							
	X	Y	X	Y	X C.P.	Y C.P.	DELTA S	SUMDS	D ALPHA	CURVATURE
43	.89481	.03961	.89481	.03961						
					.90610	.03680	.02327	.94094	-3.05235	-2.30409
44	.91731	.03370	.91731	.03370						
					.92861	.03023	.02364	.96458	-3.09626	-2.30303
45	.93981	.02646	.93981	.02646						
					.95112	.02230	.02410	.98868	-3.14792	-2.30334
46	.96231	.01783	.96231	.01783						
					.97363	.01294	.02467	1.01335	-3.22026	-2.30485
47	.98481	.00772	.98481	.00772						

DOUGLAS AIRCRAFT COMPANY
LONG BEACH DIVISION

TEST RUN CASE NO. PSF =

ON-BODY UNIFORM AXISYMMETRIC FLOW
TRANSFORMED COORDINATES

	X	Y	T1	CP	SIN A	COS A	SIGMA	N	PHI
1	.0000000	.0000000							
	.0004201	.0048879	.2125046	.9548418	.98627	.16513	-.0970273	-.0000000	.0000000
2	.0016150	.0096460							
	.0017476	.0100278	.4180400	.8252426	.94258	.33398	-.0918507	-.0000000	.0000000
3	.0018850	.0104080							
	.0041196	.0152345	.6061323	.6326036	.87443	.48515	-.0852949	.0000000	.0000000
4	.0070320	.0196850							
	.0078246	.0206965	.7809401	.3901326	.77786	.62844	-.0748195	.0000000	.0000000
5	.0086470	.0216840							
	.0137172	.0267334	.9301167	.1348830	.65728	.75364	-.0626457	.0000000	.0000000
6	.0194090	.0310700							
	.0219500	.0326914	1.0411876	-.0840716	.52032	.85397	-.0480611	.0000000	.0000000
7	.0245560	.0342060							
	.0355573	.0392697	1.1143869	-.2418583	.36657	.93039	-.0327381	.0000000	.0000000
8	.0470560	.0430710							
	.0571174	.0454812	1.1396121	-.2987157	.20346	.97908	-.0161003	.0000000	.0000000
9	.0673060	.0472790							
	.0785321	.0487123	1.1216719	-.2581479	.10703	.99426	-.0068738	.0000000	.0000000
10	.0898060	.0497010							
	.1010502	.0503457	1.0929948	-.1946377	.04613	.99894	-.0014129	.0000000	.0000000
11	.1123060	.0507400							
	.1235552	.0509499	1.0641262	-.1323645	.01364	.99991	.0010913	.0000000	.0000000
12	.1348060	.0510470							
	.1460560	.0510718	1.0411687	-.0840324	.00124	1.00000	.0015395	.0000000	.0000000
13	.1573060	.0510750							
	.1698060	.0510750	1.0269521	-.0546307	.00000	1.00000	.0009366	.0000000	.0000000
14	.1823060	.0510750							
	.1948060	.0510750	1.0197840	-.0399594	.00000	1.00000	.0005328	.0000000	.0000000
15	.2073060	.0510750							
	.2198060	.0510750	1.0155490	-.0313398	.00000	1.00000	.0003278	.0000000	.0000000
16	.2323060	.0510750							
	.2448060	.0510750	1.0127272	-.0256165	.00000	1.00000	.0002153	.0000000	.0000000
17	.2573060	.0510750							
	.2698060	.0510750	1.0107526	-.0216208	.00000	1.00000	.0001487	.0000000	.0000000
18	.2823060	.0510750							
	.2948060	.0510750	1.0093265	-.0187400	.00000	1.00000	.0001063	.0000000	.0000000
19	.3073060	.0510750							
	.3198060	.0510750	1.0082777	-.0166239	.00000	1.00000	.0000775	.0000000	.0000000
20	.3323060	.0510750							
	.3448060	.0510750	1.0075016	-.0150596	.00000	1.00000	.0000567	.0000000	.0000000
21	.3573060	.0510750							
	.3698060	.0510750	1.0069318	-.0139117	.00000	1.00000	.0000409	.0000000	.0000000
22	.3823060	.0510750							
	.3948060	.0510750	1.0065251	-.0130929	.00000	1.00000	.0000283	.0000000	.0000000

DOUGLAS AIRCRAFT COMPANY
LONG BEACH DIVISION

TEST RUN CASE NO. PSF =

ON-BODY UNIFORM AXISYMMETRIC FLOW
TRANSFORMED COORDINATES

	X	Y	T1	CP	SIN A	COS A	SIGMA	N	PHI
23	.4073060	.0510750							
	.4198060	.0510750	1.0062537	-.0125465	.00000	1.00000	.0000177	.0000000	.0000000
24	.4323060	.0510750							
	.4448060	.0510750	1.0061002	-.0122377	.00000	1.00000	.0000082	.0000000	.0000000
25	.4573060	.0510750							
	.4698060	.0510750	1.0060556	-.0121479	.00000	1.00000	-.0000007	.0000000	.0000000
26	.4823060	.0510750							
	.4948060	.0510750	1.0061176	-.0122726	.00000	1.00000	-.0000098	.0000000	.0000000
27	.5073060	.0510750							
	.5198060	.0510750	1.0062904	-.0126203	.00000	1.00000	-.0000196	.0000000	.0000000
28	.5323060	.0510750							
	.5448060	.0510750	1.0065855	-.0132144	.00000	1.00000	-.0000307	.0000000	.0000000
29	.5573060	.0510750							
	.5698060	.0510750	1.0070235	-.0140962	.00000	1.00000	-.0000442	.0000000	.0000000
30	.5823060	.0510750							
	.5948060	.0510750	1.0076369	-.0153321	.00000	1.00000	-.0000615	-.0000000	.0000000
31	.6073060	.0510750							
	.6198060	.0510750	1.0084765	-.0170249	.00000	1.00000	-.0000849	-.0000000	.0000000
32	.6323060	.0510750							
	.6448060	.0510750	1.0096224	-.0193374	.00000	1.00000	-.0001184	.0000000	.0000000
33	.6573060	.0510750							
	.6698060	.0510750	1.0112036	-.0225327	.00000	1.00000	-.0001697	.0000000	.0000000
34	.6823060	.0510750							
	.6948060	.0510750	1.0134403	-.0270613	.00000	1.00000	-.0002538	.0000000	.0000000
35	.7073060	.0510750							
	.7198060	.0510750	1.0167391	-.0337584	.00000	1.00000	-.0004028	-.0000000	.0000000
36	.7323060	.0510750							
	.7448060	.0510750	1.0219297	-.0443402	.00000	1.00000	-.0006869	.0000000	.0000000
37	.7573060	.0510750							
	.7698060	.0510750	1.0319794	-.0649814	.00000	1.00000	-.0012711	-.0000000	.0000000
38	.7823060	.0510750							
	.7935561	.0510643	1.0577859	-.1189109	-.00422	.99999	-.0018264	.0000000	.0000000
39	.8048060	.0509800							
	.8160622	.0505839	1.0821799	-.1711132	-.04693	.99890	.0028089	.0000000	.0000000
40	.8273060	.0499230							
	.8385705	.0489529	1.0852915	-.1778577	-.09876	.99511	.0082660	.0000000	.0000000
41	.8498060	.0476900							
	.8610784	.0461239	1.0748895	-.1553874	-.15057	.98860	.0133703	.0000000	.0000000
42	.8723060	.0442630							
	.8835868	.0420864	1.0545194	-.1120113	-.20243	.97930	.0181998	.0000000	.0000000
43	.8948060	.0396120							
	.9060956	.0368048	1.0238828	-.0483360	-.25429	.96713	.0227211	.0000000	.0000000
44	.9173060	.0336960							
	.9286052	.0302311	.9810611	.0375191	-.30616	.95198	.0268278	.0000000	.0000000

DOUGLAS AIRCRAFT COMPANY
LONG BEACH DIVISION

TEST RUN CASE NO. PSF =

ON-BODY UNIFORM AXISYMMETRIC FLOW
TRANSFORMED COORDINATES

	X	Y	T1	CP	SIN A	COS A	SIGMA	N	PHI
45	.9398060	.0264600							
	.9511158	.0223031	.9210497	.1516674	-.35797	.93373	.0302780	.0000001	.0000000
46	.9623060	.0178340							
	.9736278	.0129389	.8161305	.3339309	-.40986	.91215	.0329151	.0000001	.0000000
47	.9848060	.0077240							

ADDED MASS = .0000000 VOLUME = .0071425 SUM (T)(DELTA S) = 1.0212900

THE FOLLOWING NUMBERS ARE THE IMAGES THAT GET PUNCHED WHEN THERE IS PUNCHED OUTPUT

46

.00042007	.00488787	.21250456
.00174762	.01002784	.41803997
.00411964	.01523450	.60613230
.00782459	.02069655	.78094011
.01371718	.02673338	.93011668
.02194996	.03269141	1.04118760
.03555729	.03926974	1.11438695
.05711737	.04548118	1.13961208
.07853208	.04871225	1.12167194
.10105022	.05034569	1.09299484
.12355523	.05094995	1.06412616
.14605599	.05107175	1.04116875
.16980600	.05107500	1.02695213
.19480600	.05107500	1.01978402
.21980600	.05107500	1.01554903
.24480600	.05107500	1.01272725
.26980600	.05107500	1.01075259
.29480600	.05107500	1.00932650
.31980600	.05107500	1.00827771
.34480600	.05107500	1.00750165
.36980600	.05107500	1.00693183
.39480600	.05107500	1.00652514
.41980600	.05107500	1.00625370
.44480600	.05107500	1.00610024
.46980600	.05107500	1.00605564
.49480600	.05107500	1.00611760
.51980600	.05107500	1.00629039
.54480600	.05107500	1.00658552
.56980599	.05107500	1.00702345
.59480600	.05107500	1.00763687
.61980600	.05107500	1.00847654
.64480600	.05107500	1.00962242
.66980600	.05107500	1.01120362
.69480599	.05107500	1.01344031
.71980600	.05107500	1.01673909
.74480600	.05107500	1.02192967
.76980600	.05107500	1.03197938
.79355615	.05106425	1.05778587
.81606221	.05058393	1.08217986
.83857053	.04895292	1.08529155
.86107845	.04612392	1.07488951
.88358676	.04208638	1.05451944
.90609563	.03680476	1.02388279
.92860523	.03023109	.98106113
.95111584	.02230310	.92104973
.97362784	.01293890	.81613055

MATRIX SUMMATIONS FOR FINAL SOLUTIONS TOOK .000 SECONDS

NO ADDITIONAL CASES INPUT. NORMAL PROGRAM TERMINATION.

@XQT POTEN.LAMINR/ABS

I	X/L	R/L	VRATIO
1	.0000	.0000	.0000
2	.0025	.0120	.4777
3	.0050	.0167	.6477
4	.0075	.0203	.7656
5	.0100	.0232	.8360
6	.0125	.0257	.8993
7	.0150	.0278	.9474
8	.0175	.0297	.9812
9	.0200	.0315	1.0149
10	.0225	.0330	1.0441
11	.0250	.0344	1.0576
12	.0275	.0358	1.0710
13	.0300	.0370	1.0845
14	.0325	.0381	1.0979
15	.0350	.0391	1.1114
16	.0375	.0400	1.1167
17	.0400	.0409	1.1196
18	.0425	.0417	1.1225
19	.0450	.0425	1.1254
20	.0475	.0432	1.1284
21	.0500	.0438	1.1313
22	.0525	.0445	1.1342
23	.0550	.0450	1.1371
24	.0575	.0456	1.1393
25	.0600	.0460	1.1372
26	.0625	.0465	1.1351
27	.0650	.0469	1.1330
28	.0675	.0473	1.1309
29	.0700	.0477	1.1288
30	.0725	.0480	1.1267
31	.0750	.0483	1.1246
32	.0775	.0486	1.1225
33	.0800	.0489	1.1198
34	.0825	.0491	1.1166
35	.0850	.0493	1.1134
36	.0875	.0495	1.1103
37	.0900	.0497	1.1071
38	.0925	.0499	1.1039
39	.0950	.0500	1.1007
40	.0975	.0502	1.0975
41	.1000	.0503	1.0943
42	.1025	.0504	1.0911
43	.1050	.0505	1.0879
44	.1075	.0506	1.0847
45	.1100	.0507	1.0815
46	.1125	.0507	1.0783
47	.1150	.0508	1.0751

390	.9725	.0134	.8214
391	.9750	.0123	.0000
392	.9775	.0112	.0000
393	.9800	.0100	.0000
394	.9825	.0088	.0000
395	.9850	.0076	.0000
396	.9875	.0064	.0000
397	.9900	.0052	.0000
398	.9925	.0039	.0000
399	.9950	.0026	.0000
400	.9975	.0013	.0000
401	1.0000	-.0000	.0000

X/L	RHTETA	H	RDEL	LAMDA
.000	.000	2.429	.000	.0520
.002	.019	2.434	.047	.0505
.005	.028	2.451	.068	.0453
.007	.034	2.414	.081	.0566
.010	.041	2.464	.101	.0413
.012	.046	2.441	.112	.0485
.015	.051	2.500	.128	.0306
.017	.057	2.481	.140	.0362
.020	.061	2.466	.150	.0406
.022	.065	2.544	.166	.0180
.025	.071	2.533	.179	.0210
.027	.075	2.524	.190	.0238
.030	.079	2.515	.200	.0262
.032	.083	2.507	.209	.0285
.035	.087	2.500	.217	.0306
.037	.091	2.583	.236	.0074
.040	.096	2.580	.248	.0081
.042	.100	2.577	.259	.0089
.045	.104	2.574	.269	.0097
.047	.108	2.572	.279	.0104
.050	.112	2.569	.288	.0111
.052	.116	2.566	.297	.0118
.055	.119	2.564	.305	.0125
.057	.123	2.648	.325	-.0095
.060	.127	2.651	.337	-.0103
.063	.131	2.655	.348	-.0110
.065	.135	2.658	.360	-.0118
.067	.139	2.662	.371	-.0126
.070	.143	2.665	.382	-.0134
.072	.147	2.669	.393	-.0142
.075	.151	2.673	.404	-.0150
.077	.155	2.677	.415	-.0159
.080	.159	2.727	.434	-.0256
.082	.163	2.735	.446	-.0270
.085	.167	2.744	.458	-.0286
.087	.171	2.753	.471	-.0301
.090	.175	2.763	.484	-.0318
.092	.179	2.774	.496	-.0334
.095	.183	2.785	.509	-.0351
.097	.187	2.797	.522	-.0368
.100	.191	2.809	.536	-.0386
.102	.195	2.825	.550	-.0408

.105	.198	2.839	.564	-.0427
.107	.202	2.854	.578	-.0446
.110	.206	2.871	.592	-.0466
.112	.210	2.889	.607	-.0487
.115	.214	2.908	.622	-.0508
.117	.218	2.928	.638	-.0530
.120	.222	2.950	.654	-.0552
.122	.226	2.974	.671	-.0575
.125	.229	2.878	.660	-.0475
.127	.233	2.893	.674	-.0492
.130	.236	2.909	.688	-.0510
.132	.240	2.926	.702	-.0528
.135	.244	2.944	.717	-.0546
.137	.247	2.964	.732	-.0565
.140	.251	2.984	.748	-.0584
.142	.254	3.006	.764	-.0604
.145	.258	3.030	.781	-.0624
.147	.261	2.802	.731	-.0377
.150	.264	2.809	.741	-.0386
.152	.267	2.816	.752	-.0396
.155	.270	2.824	.762	-.0406
.157	.273	2.831	.772	-.0416
.160	.276	2.839	.783	-.0427
.162	.279	2.847	.793	-.0437
.165	.281	2.855	.804	-.0447
.167	.284	2.864	.814	-.0458
.170	.287	2.771	.796	-.0329
.172	.290	2.712	.785	-.0228
.175	.292	2.714	.792	-.0232
.177	.294	2.716	.800	-.0237
.180	.297	2.719	.807	-.0241
.182	.299	2.721	.814	-.0245
.185	.301	2.723	.821	-.0249
.188	.304	2.725	.828	-.0253
.190	.306	2.728	.835	-.0258
.192	.308	2.730	.842	-.0262
.195	.311	2.703	.840	-.0212
.197	.313	2.677	.837	-.0159
.200	.315	2.678	.843	-.0162
.202	.317	2.679	.849	-.0164
.205	.319	2.680	.855	-.0166
.207	.321	2.682	.861	-.0169
.210	.323	2.683	.867	-.0171
.212	.325	2.684	.872	-.0173
.215	.327	2.685	.878	-.0175
.217	.329	2.686	.884	-.0178
.220	.331	2.675	.886	-.0154
.222	.333	2.660	.886	-.0121
.225	.335	2.660	.891	-.0123
.227	.337	2.661	.896	-.0124
.230	.339	2.662	.901	-.0126
.232	.341	2.662	.907	-.0127
.235	.342	2.663	.912	-.0129
.237	.344	2.664	.917	-.0130
.240	.346	2.664	.922	-.0132
.242	.348	2.665	.927	-.0133
.245	.350	2.658	.930	-.0119

.247	.352	2.648	.931	-.0095
.250	.353	2.649	.936	-.0096
.252	.355	2.649	.940	-.0097
.255	.357	2.650	.945	-.0098
.257	.358	2.650	.950	-.0099
.260	.360	2.650	.955	-.0100
.262	.362	2.651	.959	-.0101
.265	.364	2.651	.964	-.0102
.267	.365	2.652	.969	-.0103
.270	.367	2.648	.972	-.0094
.272	.369	2.640	.973	-.0076
.275	.370	2.640	.978	-.0077
.277	.372	2.641	.982	-.0077
.280	.374	2.641	.987	-.0078
.282	.375	2.641	.991	-.0079
.285	.377	2.642	.995	-.0079
.287	.378	2.642	1.000	-.0080
.290	.380	2.642	1.004	-.0081
.292	.382	2.642	1.008	-.0082
.295	.383	2.640	1.012	-.0075
.297	.385	2.634	1.014	-.0061
.300	.386	2.634	1.018	-.0061
.302	.388	2.634	1.022	-.0062
.305	.389	2.635	1.026	-.0063
.307	.391	2.635	1.030	-.0063
.310	.392	2.635	1.034	-.0064
.313	.394	2.635	1.038	-.0064
.315	.396	2.635	1.042	-.0065
.317	.397	2.636	1.046	-.0065
.320	.399	2.634	1.050	-.0060
.322	.400	2.629	1.052	-.0049
.325	.402	2.629	1.056	-.0049
.327	.403	2.629	1.060	-.0050
.330	.404	2.629	1.064	-.0050
.332	.406	2.630	1.067	-.0050
.335	.407	2.630	1.071	-.0051
.337	.409	2.630	1.075	-.0051
.340	.410	2.630	1.079	-.0051
.342	.412	2.630	1.083	-.0052
.345	.413	2.629	1.086	-.0048
.347	.415	2.625	1.088	-.0039
.350	.416	2.625	1.092	-.0039
.352	.417	2.625	1.096	-.0039
.355	.419	2.625	1.099	-.0038
.357	.420	2.625	1.103	-.0040
.360	.422	2.625	1.107	-.0040
.362	.423	2.626	1.111	-.0040
.365	.424	2.626	1.114	-.0040
.367	.426	2.626	1.118	-.0041
.370	.427	2.625	1.121	-.0038
.372	.428	2.621	1.123	-.0029
.375	.430	2.621	1.127	-.0030
.377	.431	2.622	1.130	-.0030
.380	.433	2.622	1.134	-.0030
.382	.434	2.622	1.137	-.0030
.385	.435	2.622	1.141	-.0030
.387	.437	2.622	1.145	-.0031

.390	.438	2.622	1.148	-.0031
.392	.439	2.622	1.152	-.0031
.395	.441	2.621	1.155	-.0029
.397	.442	2.618	1.157	-.0021
.400	.443	2.618	1.160	-.0021
.402	.444	2.618	1.164	-.0021
.405	.446	2.618	1.167	-.0021
.407	.447	2.618	1.170	-.0021
.410	.448	2.618	1.174	-.0022
.412	.450	2.618	1.177	-.0022
.415	.451	2.618	1.181	-.0022
.417	.452	2.618	1.184	-.0022
.420	.453	2.618	1.187	-.0020
.422	.455	2.615	1.189	-.0013
.425	.456	2.615	1.192	-.0013
.427	.457	2.615	1.196	-.0013
.430	.458	2.615	1.199	-.0013
.432	.460	2.615	1.202	-.0013
.435	.461	2.615	1.205	-.0013
.438	.462	2.615	1.209	-.0013
.440	.463	2.615	1.212	-.0013
.442	.465	2.615	1.215	-.0013
.445	.466	2.614	1.218	-.0011
.447	.467	2.612	1.220	-.0004
.450	.468	2.612	1.223	-.0004
.452	.470	2.612	1.226	-.0004
.455	.471	2.612	1.229	-.0004
.457	.472	2.612	1.233	-.0004
.460	.473	2.612	1.236	-.0004
.462	.474	2.612	1.239	-.0004
.465	.476	2.612	1.242	-.0004
.467	.477	2.612	1.245	-.0004
.470	.478	2.611	1.248	-.0002
.472	.479	2.608	1.249	.0006
.475	.480	2.608	1.252	.0006
.477	.481	2.608	1.256	.0006
.480	.483	2.608	1.259	.0006
.482	.484	2.608	1.262	.0006
.485	.485	2.608	1.265	.0006
.487	.486	2.608	1.268	.0006
.490	.487	2.608	1.271	.0006
.492	.488	2.608	1.274	.0006
.495	.490	2.607	1.276	.0008
.497	.491	2.604	1.278	.0016
.500	.492	2.604	1.281	.0017
.502	.493	2.604	1.284	.0017
.505	.494	2.604	1.286	.0017
.507	.495	2.604	1.289	.0017
.510	.496	2.604	1.292	.0017
.512	.497	2.604	1.295	.0017
.515	.499	2.604	1.298	.0017
.517	.500	2.604	1.301	.0017
.520	.501	2.603	1.303	.0019
.522	.502	2.599	1.304	.0029
.525	.503	2.599	1.307	.0029
.527	.504	2.599	1.310	.0030
.530	.505	2.599	1.313	.0030

.532	.506	2.599	1.316	.0030
.535	.507	2.599	1.319	.0030
.537	.508	2.599	1.321	.0030
.540	.510	2.599	1.324	.0030
.542	.511	2.599	1.327	.0030
.545	.512	2.598	1.329	.0033
.547	.513	2.593	1.330	.0045
.550	.514	2.593	1.332	.0046
.552	.515	2.593	1.335	.0046
.555	.516	2.593	1.338	.0046
.557	.517	2.593	1.340	.0046
.560	.518	2.593	1.343	.0046
.563	.519	2.593	1.346	.0047
.565	.520	2.593	1.348	.0047
.567	.521	2.593	1.351	.0047
.570	.522	2.591	1.353	.0050
.572	.523	2.585	1.353	.0066
.575	.524	2.585	1.355	.0066
.577	.525	2.585	1.358	.0067
.580	.526	2.585	1.360	.0067
.582	.527	2.585	1.363	.0067
.585	.528	2.585	1.366	.0067
.587	.529	2.585	1.368	.0068
.590	.530	2.585	1.371	.0068
.592	.531	2.585	1.373	.0068
.595	.532	2.583	1.375	.0073
.597	.533	2.575	1.373	.0094

```
@PRT STAB.COEFF/FTN
FURPUR 28R2 S74R1A 10/22/82 09:56:35
SWEM*STAB(1).COEFF/FTN(48)
      IMPLICIT REAL (I-N)
      LOGICAL PFLAG
      DIMENSION COEFF(4)
      COMPLEX SIGMA(3)
      INTEGER I,IER
C THE FOLLOWING ARE THE BODY DIMENSIONS
      DATA LENGTH,DIA,CPRISM/15.5,1.58833,.8715/
      DATA TANGLE/76.25/
C THE FOLLOWING ARE THE ELLIPSOID HYDRODYNAMIC ACCESION COEFF
      DATA K1,K2,KP/.03,.96,.88/
C THE FOLLOWING ARE THE FIN COEFF.
      DATA XFIN,AFIN,ARFIN,LAMDA,SSPAN/7.111,1.667,1.504,0.,0.792/
C BODY MOMENT OF INERTIA
      DATA IYY/829.6/
      DATA PI/3.14159/
      DATA RHO,G/1.9933,32.2/
      DATA M,MAIR,ZMET/52.86,20.559,.5/
C LOOP TO TEST FOR MARGIN OF STABILITY BY INPUTING VARIABLE FIN
C AREA   10/22/82
      PFLAG=.FALSE.
      TEST=1.0
    5 AFIN=AFIN/TEST
      WRITE(6,51)
   51 FORMAT(1X,'INPUT FIN AREA FACTOR FOR TESTING STABILITY',
     1' MARGIN',/,1X,'DEFAULT IS TEST=1.0  TO STOP ENTER -1.')
      READ(5,52)TEST
   52 FORMAT(F10.0)
      IF(TEST.EQ.0.)TEST=1.0
      IF(TEST.LT.0.)STOP
      AFIN=AFIN*TEST
      FINE=LENGTH/DIA
      IPYY=IYY/(0.5*RHO*LENGTH**5)
      MP=M/(0.5*RHO*LENGTH**3)
      MTH=-MAIR*G*ZMET
      XCB=7.31
      DO 500 I=1,10
      KNOTS=FLOAT(I)/2.
      VEL=1.6889*KNOTS
      Q=0.5*RHO*VEL**2
      MPTH=MTH/(Q*LENGTH**3)
C FROM NAVORD REP 3346
      XB=(LENGTH-XCB)*(1.-0.0111*TANGLE)*0.78
      MALH=Q*LENGTH*DIA*DIA*0.25*PI*(2.0*CPRISM*(K2-K1)-(XB/LENGTH)*
     1(0.005*FINE**2+0.96*CPRISM+5.71*ABS(0.835-CPRISM)-0.012*TANGLE))
C FROM EQ 23A OF PRINC. OF NAVAL ARCH.
      CLSLOP=1.8*PI*ARFIN/((COS(LAMDA/57.296)*SQRT(ARFIN**2/COS(LAMDA
     1/57.296)**4+4.))+1.8)
      MALF=-XFIN*Q*AFIN*CLSLOP
      MAL=MALH+MALF
      MPAL=MAL/(Q*LENGTH**3)
C FROM NAVORD REP 3346
      ZALH=-Q*0.25*PI*DIA*DIA*(0.005*FINE**2+0.96*CPRISM+5.71*ABS(.835-
     1CPRISM)-0.012*TANGLE)
      ZALF=-Q*AFIN*CLSLOP
```

```
      ZAL=ZALH+ZALF
      ZPAL=ZAL/(Q*LENGTH**2)
C FROM P OF NAVAL ARCH.  EQ 56
      ZPALH=ZALH/(Q*LENGTH**2)
      ZPTHDH=-K1*MP+(XB/LENGTH)*ZPALH
      ZPALF=ZALF/(Q*LENGTH**2)
      ZPTHDF=+(XFIN/LENGTH)*ZPALF
      ZPTHD=ZPTHDH+ZPTHDF
C FROM P OF NAVAL ARCH.  EQ 58
      MPTHDH=(0.5*CPRISM)**2*ZPALH
      MPTHDF=ZPALF*(XFIN/LENGTH)**2
      MPTHD=MPTHDH+MPTHDF
C FROM P OF NAVAL ARCH.
      ZALDH=-0.25*PI*K2*RHO*CPRISM*LENGTH*VEL*DIA**2
      ZALDF=-PI*RHO*SSPAN*AFIN*VEL/SQRT(ARFIN**2+1.)
      ZALD=ZALDH+ZALDF
C THE FOLLOWING IS THE APPROX. MOMENT OF INERTIA OF DISPLACED WATER
      ZPALD=ZALD/(0.5*RHO*VEL*LENGTH**3)
      IO=IYY
      MTHDDH=-KP*IO
      MTHDDF=0.
      MTHDD=MTHDDH+MTHDDF
      MPTHDD=MTHDD/(0.5*RHO*LENGTH**5)
      IPYY=IYY/(0.5*RHO*LENGTH**5)
C CALCULATION OF POLYNOMIAL COEFF.
      COEFF(1)=(MPTHDD-IPYY)*(ZPALD-MP)
      COEFF(2)=(MPTHDD-IPYY)*ZPAL+(ZPALD-MP)*MPTHD
      COEFF(3)=ZPAL*MPTHD-(ZPTHD+MP)*MPAL+(ZPALD-MP)*MPTH
      COEFF(4)=ZPAL*MPTH
      CALL ZPOLR(COEFF,3,SIGMA,IER)
      WRITE(6,100)KNOTS
  100 FORMAT(////,1X,'STABILITY COEFF. FOR A SPEED OF',F6.2,'KNOTS')
      WRITE(6,105)SIGMA
  105 FORMAT(3(1X,'REAL PART.=',G10.4,5X,'IMAG. PART.=',G10.4/))
      IF(PFLAG)WRITE(6,600)ZALH,ZALF,ZAL,MALH,MALF,MAL
  600 FORMAT(/,1X,'ZALH=',F10.4,'  ZALF=',F10.4,'  ZAL=',F10.4,/
     11X,'MALH=',F10.4,'  MALF=',F10.4,'  MAL=',F10.4)
      IF(PFLAG)WRITE(6,700)ZPAL,MPTHD,ZPTHD,MP,MPAL
  700 FORMAT(/,1X,'ZPAL=',G10.4,'  MPTHD=',G10.4,'  ZPTHD=',G10.4,/
     1,1X,'MP=',G10.4,'  MPAL=',G10.4)
      MPALH=MALH/(Q*LENGTH**3)
      MPALF=MALF/(Q*LENGTH**3)
      IF(PFLAG)WRITE(6,805)MPALH,MPALF
  805 FORMAT(/,1X,'MPALH=',G10.4,'MPALF=',G10.4)
      IF(PFLAG)WRITE(6,800)COEFF(1),COEFF(2),COEFF(3),COEFF(4)
  800 FORMAT(/,1X,'A=',G10.4,' B=',G10.4,'  C=',G10.4,'  D=',G10.4)
  500 CONTINUE
      GO TO 5
      END
```

```
@XQT STAB.COEFF/ABS
INPUT FIN AREA FACTOR FOR TESTING STABILITY MARGIN
DEFAULT IS TEST=1.0  TO STOP ENTER -1.
```

```
STABILITY COEFF. FOR A SPEED OF   .50KNOTS
REAL PART.=-1.092          IMAG. PART.= 8.327
REAL PART.=-1.092          IMAG. PART.=-8.327
REAL PART.=-.6480          IMAG. PART.= .0000

STABILITY COEFF. FOR A SPEED OF  1.00KNOTS
REAL PART.=-1.077          IMAG. PART.= 3.963
REAL PART.=-1.077          IMAG. PART.=-3.963
REAL PART.=-.6775          IMAG. PART.= .0000

STABILITY COEFF. FOR A SPEED OF  1.50KNOTS
REAL PART.=-1.045          IMAG. PART.= 2.398
REAL PART.=-1.045          IMAG. PART.=-2.398
REAL PART.=-.7421          IMAG. PART.= .0000

STABILITY COEFF. FOR A SPEED OF  2.00KNOTS
REAL PART.=-.9675          IMAG. PART.= 1.499
REAL PART.=-.9675          IMAG. PART.=-1.499
REAL PART.=-.8975          IMAG. PART.= .0000

STABILITY COEFF. FOR A SPEED OF  2.50KNOTS
REAL PART.=-1.401          IMAG. PART.= .0000
REAL PART.=-.7159          IMAG. PART.= .8904
REAL PART.=-.7159          IMAG. PART.=-.8904

STABILITY COEFF. FOR A SPEED OF  3.00KNOTS
REAL PART.=-1.902          IMAG. PART.= .0000
REAL PART.=-.4651          IMAG. PART.= .6717
REAL PART.=-.4651          IMAG. PART.=-.6717

STABILITY COEFF. FOR A SPEED OF  3.50KNOTS
REAL PART.=-2.145          IMAG. PART.= .0000
```

```
REAL PART.=-.3439          IMAG. PART.= .5628
REAL PART.=-.3439          IMAG. PART.=-.5628


STABILITY COEFF. FOR A SPEED OF  4.00KNOTS
REAL PART.=-2.283          IMAG. PART.= .0000
REAL PART.=-.2749          IMAG. PART.= .4871
REAL PART.=-.2749          IMAG. PART.=-.4871


STABILITY COEFF. FOR A SPEED OF  4.50KNOTS
REAL PART.=-2.370          IMAG. PART.= .0000
REAL PART.=-.2311          IMAG. PART.= .4297
REAL PART.=-.2311          IMAG. PART.=-.4297


STABILITY COEFF. FOR A SPEED OF  5.00KNOTS
REAL PART.=-2.430          IMAG. PART.= .0000
REAL PART.=-.2012          IMAG. PART.= .3842
REAL PART.=-.2012          IMAG. PART.=-.3842

INPUT FIN AREA FACTOR FOR TESTING STABILITY MARGIN
DEFAULT IS TEST=1.0  TO STOP ENTER =1.
```